WETTABILITY EVALUATION OF ROCKS USING NMR

BY

KAREM ABDULRAHMAN AL-GARADI

A Thesis Presented to the
DEANSHIP OF GRADUATE STUDIES

KING FAHD UNIVERSITY OF PETROLEUM & MINERALS
DHAHRAN, SAUDI ARABIA

In Partial Fulfillment of the
Requirements for the Degree of

MASTER OF SCIENCE

In

PETROLEUM ENGINEERING

DECEMBER 2019

KING FAHD UNIVERSITY OF PETROLEUM & MINERALS

DHAHRAN- 31261, SAUDI ARABIA

DEANSHIP OF GRADUATE STUDIES

This thesis, written by **KAREM ABDULRAHMAN AL-GARADI** under the direction of his thesis advisor and approved by his thesis committee, has been presented and accepted by the Dean of Graduate Studies, in partial fulfillment of the requirements for the degree of **MASTER OF SCIENCE IN PETROLEUM ENGINEERING.**

Dr. Mohamed Mahmoud
(Advisor)

Dr. Dhafer A. Al Shehri
Department Chairman

Dr. Ammar Elhusseiny
(Co-Advisor)

Dr. Salam A. Zummo
Dean of Graduate Studies

Dr. Salaheldin Elkatatny
(Member)

24/12/19
Date

Dr. Abdulrauf Adebayo
(Member)

Dr. Michael Johns
(Member)

This work is dedicated to my beloved father

ACKNOWLEDGMENTS

All thanks and praise to Almighty Allah for giving me knowledge, determination, health and patience to complete this work successfully. I would like to express my deep thanks to King Fahd University of Petroleum and Minerals (KFUPM), namely, Petroleum Engineering Department for offering a scholarship to me to complete both my bachelor and master's degrees. Special thanks go to College of Petroleum Engineering & Geosciences (CPG) for supporting me during my master's degree.

I would like to express my highly appreciation and great thanks to my advisor Dr. Mohamed Mahmoud for his support, guidance, effort, time, and valuable comments. In addition, my deep thanks go to my co-advisor Dr. Ammar Elhusseiny for his guidance, time, and valuable comments. I also thank Dr. Hasan Al-Yousef for his valuable comments and guidance. My great thanks go to my committee members Dr. Michael Johns, Dr. Abdulrauf Adebayo, and Dr. Salaheldin Elkatatny for their valuable contribution.

I would like to thank Center of Integrative Petroleum Research (CIPR) for allowing me to use the labs and facilities during my research. Special thanks go to Dr. Abdulrauf Adebayo, Mr. Rahul Babu, Mr. Syed Hussaini, Mr. Sarmad Khan, Mr. Abdulsamad Iddrisu, Mr. Jafar Al Hamad, Mr. Abdelmjeed Mohamed, and Mr. Abdulrahim Muhammadain for helping me in during my work.

My thanks go to University of Western Australia (UWA) for hosting me for two months during which I was trained on the use of specialist NMR techniques for analysis of reservoir

rock cores and fluids (Petrophysics). I would like to thank Dr. Paul Connolly, Dr. Michael Johns and Dr. Nicholas Ling for training me and for their valuable contribution to this work.

My deep thankfulness, gratitude, and appreciation go to my father, who died during my last year of bachelor's degree, for his indescribable support, encouragement and prayers. I would also like to express my great thanks and gratitude to my wife, mother, brothers, and sisters for their encouragement and prayers.

Finally, I would like to thank my friends, colleagues. Special thanks go to Mr. Akram Al-Absi, Mr. Ayman Alazab, Mr. Qais Jawah, Mr. Nadhem Ismail, Mr. Anwar Aljaml, Mr. Hamza Abulhoom, Mr. Omar Alazab, and Mr. Yousef Alwajeeh.

TABLE OF CONTENTS

LIST OF TABLES

LIST OF FIGURES

LIST OF ABBREVIATIONS

NMR	:	Nuclear Magnetic Resonance
USBM	:	US Bureau of Mines
CPMG	:	Carr-Purcell-Meiboom-Gill
XRD	:	X-Ray Diffraction
HTS	:	Hexadecyl-trimethoxy-silane
IR	:	Inversion Recovery
IRSE	:	Inversion Recovery Spin Echo
SD	:	Silurian Dolomite
EB	:	Edward Brown Carbonate
UWA	**:**	University of Western Australia

ABSTRACT

Full Name : [Karem Abdulrahman Al-Garadi]

Thesis Title : [Wettability Evaluation of Rocks Using NMR]

Major Field : [Petroleum Engineering]

Date of Degree : [December 2019]

Understanding reservoir behaviors is crucial to maximize its production effectively. Different technologies, methods, and tools are used to analyze and characterize reservoir rocks, fluids, and rock/fluid interactions. Nuclear magnetic resonance (NMR) has become an important tool in oil and gas industry. Furthermore, in formation evaluation, NMR wireline logs have become a cornerstone. NMR has a variety of applications in oil and gas industry. For example, different petro-physical parameters are determined and assessed by NMR such as, wettability.

In this work, NMR measurements were used to evaluate the wettability of different rocks. Two different approaches were followed to establish rock samples with different wettability conditions. In the first approach, Silurian dolomite (SD) and Edward Brown (EB) carbonate samples, that are originally water wet, were chemically treated by Hexadecyl-trimethoxy-silane (HTS) to alter their wettability into oil-wet condition. T_2, T_1T_2 NMR measurements were conducted before and after the treatment at two situations, which are fully brine saturated and paraffin oil/brine saturated conditions. In addition, ultrasonic velocity measurements were also conducted since the NMR core holder

developed in UWA has the ability to run NMR and ultrasonic velocity measurements together. In the second approach, T_2 and T_1T_2 NMR measurements were conducted on carbonate rocks that were aged in actual crude oil containing asphaltene and non-aged sandstone samples saturated with brine and actual crude oils with different asphaltene content at different saturations.

The current methods of wettability evaluation have many limitations. For example, they are time consuming, and laboratory based tests. NMR can be a good candidate to replace the current methods of wettability measurement especially that it can be applied in-situ at the field. However, there are few studies on how to quantify wettability using NMR measurements especially in carbonate rocks where they face some critical challenges due to the pore complexity of carbonates. All the above motivates us to conduct this research in order to develop an approach to evaluate wettability of rocks with various pore complexity and geometry (from sandstone to carbonate) based on NMR measurements.

In this work, T_2 and T_1T_2 NMR measurements were used to assess rock wettability. NMR T_2 measurements determined rock wettability conditions very well in the second approach but they did not work well in the first approach due to two main reasons. The first reason is that the treatment method failed because it was not done properly. The second one is that the measurements were not conducted at the two extreme saturations (irreducible water and residual oil saturations) which made the separation of oil and water signals a must in order to assess wettability. T_1T_2 measurements for the two approaches needed the separation of oil and water signals by any technique such as T_2-D NMR measurements in order to extract wettability information from T_1/T_2 ratio especially in the second approach where we used actual crude oils. NMR measurements are easier to obtain, and save much more time and

effort compared to the available conventional methods. NMR technology can be extended to be applied in the field, which would be very commercial and economically feasible.

ملخص الرسالة

الاسم الكامل: كريم عبدالرحمن الجرادي

عنوان الرسالة: تقيم نوع ودرجة تبليل أو ترطيب الصخور بإستخدام الرنين المغناطيسي النووي

التخصص: هندسة البترول

تاريخ الدرجة العلمية: ديسمبر ٢٠١٩

فهم طبيعة وسلوكيات خزان النفط أو الغاز أمر بالغ الأهمية لزيادة إنتاجه بشكل فعال. تُستخدم تقنيات وأساليب وأدوات مختلفة لتحليل وتوصيف صخور وموائع الخزان وتفاعلات الصخور مع الموائع. أصبح الرنين المغناطيسي النووي أداة مهمة في مجال صناعة النفط والغاز. علاوة على ذلك ، في تخصص دراسة تكوين الخزان ، أصبح الرنين المغناطيسي النووي حجر أساس. الرنين المغناطيسي النووي لديه مجموعة متنوعة من التطبيقات في صناعة النفط والغاز. على سبيل المثال ، يتم تحديد خواص الخزان البتروفيزيائية المختلفة وتقييمها بواسطة الرنين المغناطيسي النووي مثل نوع ودرجة تبلل الصخور.

في هذا العمل ، استخدمت قياسات الرنين المغناطيسي النووي لتقييم درجة رطوبة الصخور المختلفة. تم إتباع طريقتين مختلفتين لإنشاء عينات صخور ذات درجات تبلل مختلفة. في النهج الأول ، عولجت كيميائيًا عينات من الصخور الكربونية التي هي في ألاصل مبللة بالماء ، لتحويلها الى صخور مبللة بالزيت. أجريت قياسات قياسات الرنين المغناطيسي النووي قبل وبعد العلاج على خطوتين ، وهي عبارة عن العينات مشبعة بالكامل بمحلول ملحي وبعد ذلك العينات مشبعة بالزيت و المحلول ملحي معاً. في الطريقة الثانية أجريت قياسات قياسات الرنين المغناطيسي النووي على عينات من الصخور الرملية و الصخور الكربونية المشبعة بالمحلول الملحي و الزيوت الخام ذات محتوى مختلف من الأسفلت في درجات تشبع مختلفة.

الطرق المستخدمة حالياً لتقييم درجة تبليل الصخور لها العديد من القيود. على سبيل المثال ، هذه الطرق تستهلك الكثير من الوقت كما أنه لا يمكن تطبيقها إلا في المعامل والمختبرات فقط. الرنين المغناطيسي النووي يمكن أن يكون بديلاً ممتازاً لهذه الطرق خاصة أنه يمكن تطبيقه في حقل النفط مباشرة. مع ذلك ، هناك دراسات قليلة عن طرق القياس

الكمي لدرجة رطوبة الصخور باستخدام الرنين المغناطيسي النووي خاصة في الصخور الكربونية ذات الهيكل والخواص المعقده. كل ما سبق ذكره شجعنا للقيام بهذا البحث لتطوير طريقة جديدة تقوم بتقييم درجة ونوع رطوبة الصخور خاصة الكربونية باستخدام الرنين المغناطيسي النووي.

في هذا البحث ، أجريت قياسات الرنين المغناطيسي النووي على عينات مختلفة من الصخور لتقييم درجة ونوع رطوبتها. قياسات الرنين المغناطيسي النووي قامت بتقييم نوع ودرجة التبلل بشكل جيد للغاية في النهج الثاني لكنها لم تعمل بشكل جيد في النهج الأول لأن طريقة العلاج الكيميائي للصخر فشلت حيث أنها لم تتم بالشكل الصحيح. الرنين المغناطيسي النووي يقيم درجة تبليل الصخور ويعطي قياسات ونتائج دقيقة كما أنه يوفر الوقت والمال ولا يفسد عينات الصخور. يمكن توسيع تكنولوجيا الرنين المغناطيسي النووي ليتم تطبيقها في حقول النفط والغاز، الأمر الذي سيكون تجاريًا جدًا ومجديًا اقتصاديًا.

CHAPTER 1

INTRODUCTION

1.1 Background

The tendency of a fluid to preferentially wet a solid surface in the presence of other immiscible fluids is defined as wettability [1]. Wettability is a critical input parameter in reservoir description and simulation [2]. This is because wettability strongly influences important reservoir quantities and parameters such as relative permeability, residual oil saturation and capillary pressure curves [3]–[5]. Reservoir electrical properties are also influenced by wettability [6]–[10]. It also controls the flow in the pore space and fluid distribution [4], [5], [11]–[13], which in turns impact the hydrocarbon recovery.

Rocks wettability could be divided into four main categories [14], which are oil wet, water wet, mixed wettability and fractional wettability. Water wet rocks means that the rock surface is preferentially in contact with water while the rocks that are oil wet tend to preferentially contact oil, so their surfaces are coated by oil. Fraction wettability is where portions of the rock are strongly water wet while the rest are oil wet. Fraction wettability exists because rock mineralogy varies through the reservoir casing a variation in surface chemical properties. Mixed wettability means that the water fills the smaller pores and wets them while the larger pores contain oil and water with portion of them is wetted by oil. This is usually attributed to the oil composition such that crude oil containing resins and asphaltenes has surface-active polar molecules that are

attracted to opposite charge sites on the pore surfaces which alters the wettability. Asphaltenes and resins have large molecule sizes which cannot enter the smaller pores causing wettability alterations.

Direct measurement of reservoir wettability is still a challenge. Preserving the original wettability conditions for a core sample is almost impractical. The variation between the surface and reservoir conditions and the contamination caused by drilling fluids are some examples that could change the in-situ wettability [15].

According to Minh, et al. [16], the existing methods of wettability measurements can be divided into two groups. The basis of first group methods is capillary pressure observing during drainage and imbibition [11], [17] or the phenomenon of spontaneous imbibition [2]. Group two techniques deduce the relative contact contributions of fluids to the total surface area utilizing NMR measurements [18]–[27] or contact angle microscopy [28].

Amott [17] and USBM [11] are very common tests for wettability measurement. However, they are time consuming and can only be carried out in the laboratory. Moreover, they do not frequently give consistent results [18]. In addition, they require thorough cleaning of the core sample and restoration of original in-situ wettability condition, which can be very challenging. Both Amott and USBM firstly require injecting oil into a fully water saturated sample until initial water saturation S_{wi} is achieved and then aging for some time at high temperature value. This step is significant since the measurements final result is strongly dependent on S_{wi} value and temperature [29].

Nuclear Magnetic Resonance (NMR) logging has increasingly become more significant in oil industry [30]. NMR presents a relatively fast approach for evaluation of various petro-physical

rock properties including pore sizes, porosity, permeability, and free fluid index [30], [31]. Recently, more studies started to look into the use of NMR for more advanced application including the evaluation of pore geometry complexity [32]–[40] and wettability [17], [20], [33], [46], [41]–[45].

In sandstone rocks, NMR has been proved as an efficient tool for different applications. However, there are many challenges facing NMR measurements on carbonate rocks [47]. Carbonate rocks, unlike sandstone have totally different and more complicated pores system and it is difficult to correlate their petrophysical properties such as permeability and porosity. Diagenesis process results in reorganization of porosity leading to this behavior and imposes many challenges on reservoir quality prediction of carbonate rocks [47].

1.2 NMR Theory

Nuclear magnetic resonance (NMR) is a phenomenon that occurs when atomic nuclei response to magnetic fields [48]. Some nuclei behave like spinning bar magnets since they have a property called magnetic moment as shown in Figure 1. When applying an external magnetic field, the nuclei will interact and a measurable signal is produced. Hydrogen nucleus is an example and it has a relatively large magnetic moment [31]. The pore space contains water and hydrocarbon, which consist of hydrogen atoms in their molecular structure. Applying a static magnetic field followed by a series of radio frequency pulses excites the hydrogen atoms and valuable information are obtained once they return to their original state [30], [31]. Based on the type of the radio frequency pulses, different NMR parameters are measured.

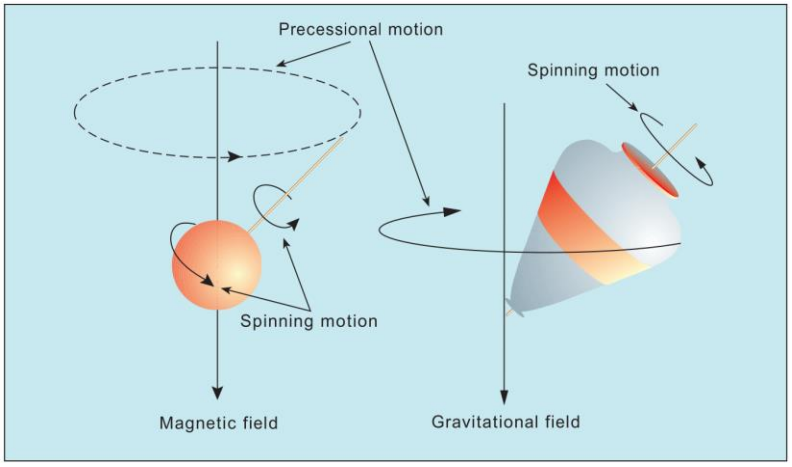

Figure 1 Some nuclei acts like spinning bar magnates. Applying a static magnetic field causes the nuclei to precess around it [31].

1.2.1 T_2 Measurements

Spin-spin relaxation decay or T_2 relaxation time is an important parameter measured from NMR experiments. T_2 describes the decay of NMR signal in the transverse plane, which is controlled by three different factors/mechanisms, as highlighted by Eq. 1:

$$\frac{1}{T_2} = \frac{1}{T_{2,bulk}} + \frac{1}{T_{2,surface}} + \frac{1}{T_{2,diffusion}} \quad (1)$$

The first term in Eq. 1 ($T_{2,\text{ bulk}}$) describes the effect of bulk fluid properties (mainly viscosity) on the relaxation time. The second term ($T_{2,\text{ surface}}$) is related to the solid surface chemistry and geometry. Surface interactions reduce T_2 to shorter times so the wetting phase inside a pore space would have shorter T_2 compared to that of bulk fluid [22]. The last term ($T_{2,\text{diffusion}}$) corresponds to the impact of magnetic field inhomogeneity; T_2 is sensitive to changes in the individual spins position, and hence to the sample diffusivity [49]. Diffusion reduces echo amplitude resulting in shorter T_2 times [30].

Carr-Purcell-Meiboom-Gill (CPMG) pulse sequence [50], [51] is commonly used to measure T_2. This sequence minimizes the effect of field inhomogeneity so that the relaxation from diffusion is negligible and the last term in Eq. 1 is cancelled as shown in Eq. 2. CPMG is the pulse sequence used for all T_2 measurements in this research.

$$\frac{1}{T_2} = \frac{1}{T_{2,bulk}} + \frac{1}{T_{2,surface}} \tag{2}$$

Figure 2 represents the standard CPMG pulse sequence. In CPMG sequence, a 90^o pulse is applied followed by a series of 180^o pulses. After each 180^o pulse, the signal is acquired and it represents an echo [30]. T_E is the time spacing between the 90^o pulse and the first echo and it should be short enough to minimize the effects of gradient on T_2 so the last term in Eq. 3 becomes negligible [49].

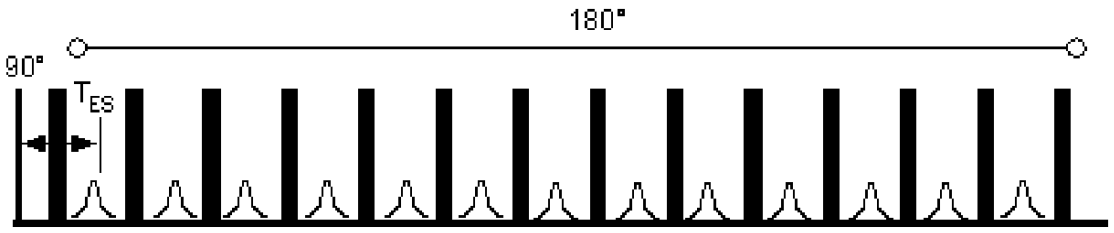

Figure 2 Standard CPMG pulse sequence [49]

1.2.2 T_1T_2 Measurements

T_1 relaxation time or spin-lattice relaxation decay is another important parameter in NMR that describes the decay of NMR signal in the longitudinal plane. T_1 measurements consume more

time than T_2 because they require waiting for polarization [41]. Unlike T_2, T_1 is not affected by diffusion and it is controlled only by bulk and surface relaxations, as shown in Eq. 2:

$$\frac{1}{T_1} = \frac{1}{T_{1,bulk}} + \frac{1}{T_{1,surface}} \quad (2)$$

Inversion recovery (IR) pulse-sequence, shown in Figure 3, is used to measure T_1. In inversion recovery sequence, a 180^o pulse is applied followed by a 90^o pulse. After the 90^o pulse, the signal is acquired. τ or sometimes called TI is the time spacing between the 180^o pulse and the 90^o pulse.

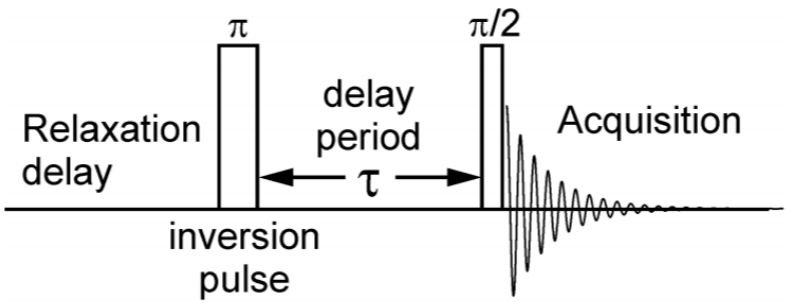

Figure 3 Inversion recovery pulse-sequence [52]

Individual measurements of T_1 or T_2 is referred as 1D NMR distribution [30]. However, a full T_2 decay signal could be acquired for each wait time (TI or τ) during the T_1 acquisition, and thus a 2D dataset can be generated with T_1 and T_2 data [30]. Figure 4 shows the inversion recovery spin echo (IRSE) sequence used to obtain 2D dataset with T_1 and T_2 data. The sequence consist of two parts. The first part represents inversion recovery sequence while the second part is the CPMG sequence (series of 180^o pulses after the 90^o pulse).

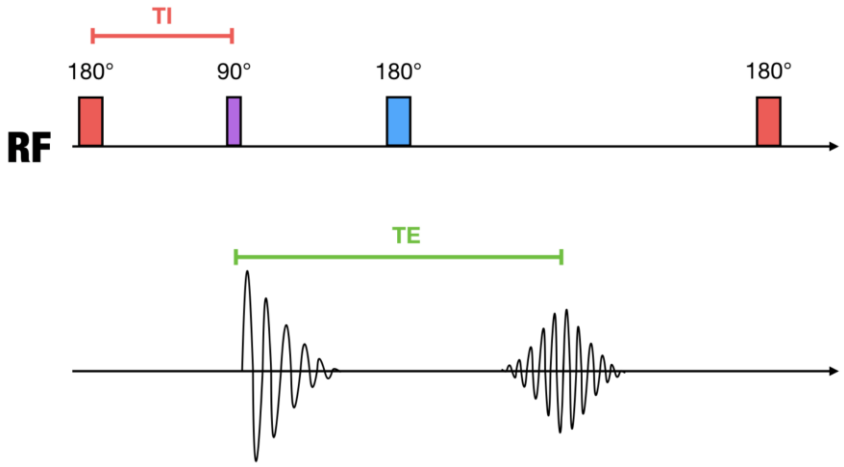

Figure 4 Inversion recovery spin echo pulse sequence [53]

2D maps are generated from the T_1T_2 measurements as the one shown in Figure 5, which represents T_1T_2 map of a bulk water sample. T_1 and T_2 are equal for bulk, non-viscous fluids where the molecules motion is fast and isotropic which is the case for water and light oil [41], [54]. This means that bulk fluids usually locate on the unity line ($T_1/T_2 = 1$). Inside a pore space, T_1/T_2 ratio of non-wetting phase deviates from unity since the molecules motion becomes anisotropic so T_1 and T_2 are affected in different ways [41], [54].

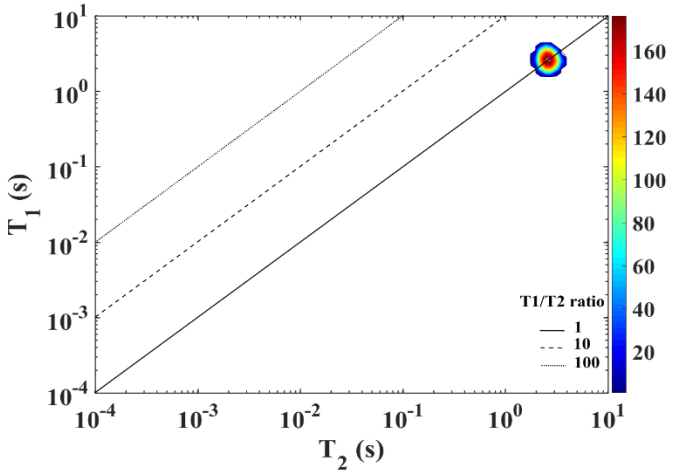

Figure 5 T_1T_2 map of bulk water

CHAPTER 2

LITERATURE REVIEW

2.1 Traditional Approaches for Wettability Evaluation

2.1.1 Amott-Harvey Test

Amott test set-up is shown in Figure 6. In Amott-Harvey test, the sample, that has been aged and saturated with oil/water at S_{wi}, is immersed in water and the produced oil volume by spontaneous imbibition of brine (V_{o1}) is measured. Then, water is forced into the sample by centrifuge [17] or water-flooding [55] and additional produced oil volume (V_{o2}) is recorded. After that, the sample is immersed in oil and spontaneous produced water volume (V_{w1}) is measured. Finally, oil is forced into the sample by centrifuge or oil injection and additional produced water volume (V_{w2}) is recorded. Amott-Harvey index is defined in Eq. 3.

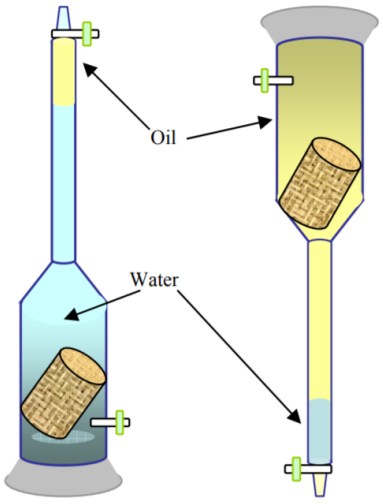

Figure 6 Amott test set-up [56]

$$I_{AH} = I_w - I_o = \frac{V_{o1}}{V_{o1}+V_{o2}} - \frac{V_{w1}}{V_{w1}+V_{w2}} \quad (3)$$

Where, I_{AH} is the Amott-Harvey wettability index, I_w is the Amott water wettability index, and I_o is the Amott oil wettability index. I_{AH} ranges from -1 to 1. For strongly water wet system, almost all the oil is produced from the spontaneous imbibition by brine ($V_{o2} \approx 0$) which makes $I_w \approx 1$ and no water is produced from the spontaneous imbibition by oil ($V_{w1} \approx 0$) which makes $I_o \approx 0$ so the Amott-Harvey index is equal to 1. On the other hand, strong oil wet systems have I_{AH} close to -1. Table 1 shows the wettability classification based Amott-Harvey index [55]. The main disadvantage of the Amott method is that it takes long time that can exceed a month [15].

Table 1 Wettability characterization based on Amott-Harvey index

I_{AH}	Wettability Type
-1 to -0.3	Oil wet
-0.3 to 0.3	Intermediate Wet
0.3 to 1	Water wet

2.1.2 USBM Wettability Index

The USBM method uses the centrifuge to imbibe water into the rock (imbibition) that is aged and saturated with oil/water at S_{wi}. Then, oil is forced into the rock by centrifuge (drainage). The capillary pressure curves for the two cycles (imbibition and drainage) are constructed. The

area under the capillary pressure curves is used to calculate the wettability index as shown in Eq. 4.

$$I_{USBM} = \log\frac{A_1}{A_2} \tag{4}$$

Where, I_{USBM} is the USBM wettability index, A_1 and A_2 correspond to the area under the drainage and imbibition curve, respectively as shown in Figure 7. USBM test is faster than Amott method but saturations have to be corrected due to the nonlinear capillary pressure gradient effect [15]. In addition, USBM method is not reliable in neutral or mixed wet systems [15]. Finally, the centrifuge could damage the rock so USBM method is not recommended for soft rocks [15].

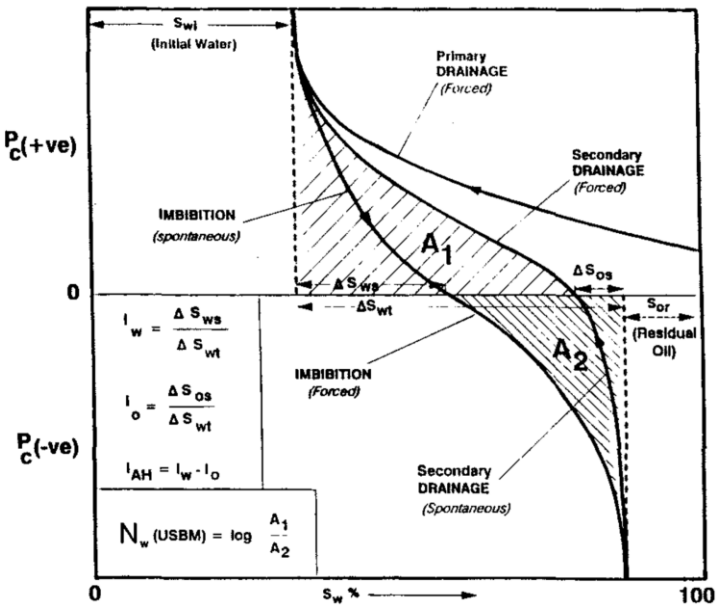

Figure 7 Amott and USBM indices [57]

2.2 NMR As a Potential Tool for Wettability Evaluation

Freedman et al. [22], [58] presented how NMR T_2 measurements could evaluate wettability qualitatively. NMR measurements on oil/water saturated pore system have sensitivity to wettability due to the enhancement of relaxation rate (shorter T_2 time) when wetting fluid contacts pore surfaces. The dominant relaxation mechanism for the wetting phase is the surface relaxation while the non-wetting fluid is not significantly influenced by surface relaxation since it does not coat or contact pore surfaces [22]. In this case, the non-wetting fluid inside the pores shows bulk and diffusion relaxations only, and consequently it tends to behave like bulk fluid [22]. The surface relaxation is also influenced by the wetting phase saturation as we see in Eq. 5 [22]. At lower wetting fluid saturations, the shift of T_2 to shorter times due to surface relaxation is more pronounced relative to that at higher saturations [22].

$$\frac{1}{T_{2,surf}} = \frac{\rho A_S}{V_p S_f}, \tag{5}$$

Where, ρ is the surface relaxivity, A_S is the pore surface area contacted by the wetting fluid, V_p is the pore volume, and S_f is the wetting phase saturation.

Looyestijn et al. [59], [60] introduced a quantitative wettability index from NMR. The model was developed based on the fact that additional relaxation is experienced by wetting fluids contacting the rock surface directly, compared to non-wetting fluids that shows only bulk relaxation. When compared with USBM, NMR approach could provide reasonable prediction in carbonates of relatively low permeability (few mD) when using 20 cp oil viscosity [59], [60]. Nevertheless, the accuracy of the approach decreases with increasing oil viscosity and increasing pore-sizes [59], [60]. Additionally, this approach requires a pore-size dependent

fluid saturation distribution [59], [60], which can be challenging to obtain in rocks with complex pore geometry.

Al-Mahrooqi et al. [61] proposed a simple pore-scale model to evaluate wettability based on T_2 measurements. The model consist of a bundle of capillary tubes with a triangular cross section, and it was used to investigate the relationship between wettability and NMR relaxation times. Based on the experimental and modelling results, the authors observed that T_2 values at residual and irreducible saturation are sensitive to the same amounts used to compute the Amott–Harvey index. The model was tested against known wettability synthetic samples and real sandstone samples having various wettabilities.

Branco et al. [15] used Al-Mahrooqi et al. [61] model to calculate wettability index for carbonate rocks. The results were compared with the Amott-Harvey index. Results obtained from Al-Mahrooqi index did not agree with that obtained from Amott-Harvey index and this was attributed to the pore coupling effect.

T_1T_2 maps were also used to evaluate rock wettability [41], [54]. Bulk fluids usually has T_1/T_2 ratio equal to one. When fluids are inside the pore space, the T_1/T_2 ratio of the wetting phase deviates from unity while the non-wetting phase shows T_1/T_2 close to one like the bulk fluid. However, this technique has a major limitation such that the oil T_1/T_2 ratio may deviate from unity due to intrinsic bulk oil properties [41]. Relating this deviation to wettability would result in wrong conclusions.

Minh, et al. [16] exploit the 2D mapping of (T_2-D) to derive wettability index used to characterize rocks wettability. This method produces more accurate wettability values than the T_2-based methods do since it provides better and improved separation of the water and oil

signals. In addition, using restricted diffusion models, the T_2-D maps are used to deduce effective surface relaxivity based on it, wettability index is determined. Fresh- state plugs obtained from coring with water-base muds containing no surfactants were used to conduct the NMR measurements. The NMR wettability indices showed an agreement with the USBM indices with a correlation coefficient R^2 equal to 0.7.

2.3 Wettability Alteration Mechanisms

Asphaltene is considered as the heaviest component in crude oil that is soluble in aromatic solvents but insoluble in normal alkanes [62]. It was observed in different studies that Asphaltene adsorbtion altered rock wettability to mixed or oil wet [13], [42], [70]–[74], [43], [63]–[69]. In addition, Asphaltene precipitation is one of the main mechanisms of altering rock wettability towards mix or oil wet and it is more likely to occur when changing temperature and pressure conditions such as the aging process [64]. Asphaltene represents the major component of crude oil causing wettability alteration in carbonate reservoirs [66]. The adsorption of polar organic components of crude oil such as asphaltene on the carbonate rock surface alter their wettability from originally water-wet to oil wet condition [63], [66]–[70]. Outcrop carbonates are generally water wet but it is observed that most carbonate reservoirs are neutral to oil wet [67], [71]. Johansen et al. [72] showed that some water/oil/glass systems were water wet when using deasphalted oil but wettability was altered to oil wet when a very small amount (0.25%) of the asphalted crude oil was added to the deasphalted oil. Strassner [75] showed that the oil wetness of a glass surface increased with increasing oil asphaltene content.

By adding 0.12 wt% of asphaltene in toluene and then aging, the wettability of fresh calcite surfaces that are pre-wetted in deionized water changed from water to intermediate or oil wet conditions due to asphaltene amphiphilic property that leads to high interaction with calcite surface creating an oil-wet surface [66]. Tabrizy et al. [73] also investigated the asphaltene role in wetiiblity modification of calcite and other minerals. They added 0.35 wt% of asphaltene to toluene in addition to 0.01 M solution of stearic acid and N,N-dimethyldodecylamine. They noticed that asphaltene and stearic acid deeply altered the calcite toward more oil-wet. Tipura [56] used some limestone core plugs that are originally strong water wet to age them at S_{wi} with different oil samples (different asphaltene content) at various times. Most of the aged samples showed mix-wet conditions and some showed oil wet conditions. Al-Aulaqi [74] studied different methods for wettability alteration. He concluded that asphaltene content is a significant crude oil component causing wettability alteration of solid surface to intermediate or oil wet. He also found that the removal of crude oil asphaltene reduces the oil-wetness and the temperature does not create major wettability change of deasphalted oil compared to asphalted one. Gizatullin et al. [43] aged chalk, Bentheimer and Berea with a bitumen solution converting their wettability from water to mixed-wet.

Shikhov et al. [42] used NMR T_2 relaxation times to qualitatively monitor asphaltene adsorption and wettability alteration of Bentheimer sandstone samples when aged in oil with variable asphaltene content ranging from 1.23 to 6.56 wt%.

Chemical treatment also alters rock wettability. Hexadecyl-trimethoxy-silane (HTS) alter rocks wettability into oil wet. Reaction of HTS with surface hydroxyl species. Alkane chain creates oil affine surface as shown in Figure 8.

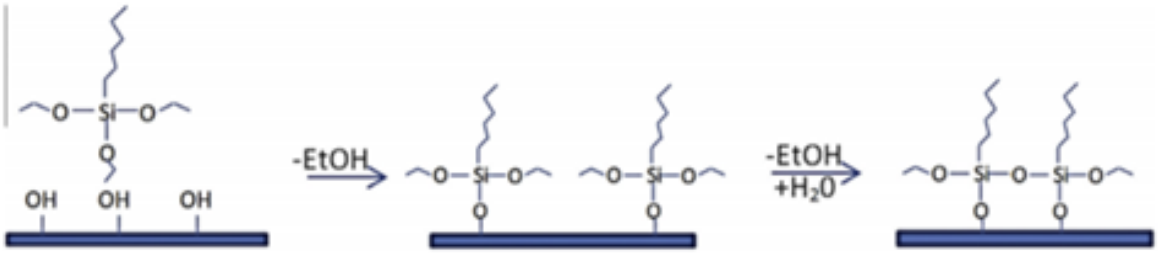

Figure 8 Reaction of HTS with surface hydroxyl species. Alkane chain creates oil affine surface

CHAPTER 3

MATERIALS AND METHODOLOGY

The materials used and the followed methods in this research are discussed in this section. It provides fluids, rocks, and chemicals types & properties in addition to the equipment used. Furthermore, the detailed methodology for achieving the research objectives is discussed.

3.1 First Approach: Wettability Alteration by Chemical Treatment

This approach is based on using chemical treatment to alter the wettability of rocks and conducting T_2 and T_1T_2 NMR measurements before and after the treatment to evaluate rocks wettability. In addition, ultrasonic velocity measurements were conducted before and after the treatment since the experimental set up developed in UWA allows NMR and ultrasonic measurements to be conducted together [76]. Detailed explanation of materials and methods used in this approach is provided below.

3.1.1 Materials and Equipment

Two samples were used in this part of the research. Silurian dolomite (SD) and Edward Brown (EB) carbonate are the two samples. 1 % NaCl brine and paraffin oil are the fluids used in this part of the study. Hexadecyltrimethoxysilane (HDS) surfactant is the chemical used to alter rock wettability. The confining fluid is (Fluorinert^{TM} FC-70) which is an NMR inert fluorocarbon oil.

Figure 9 shows the experimental set up used in this part of the research. It consist of the following parts:

1. The Magritek 2 MHz Rock Core Analyzer that was used to conduct NMR measurements.
2. Modified FCH NMR comparable core holder as shown in Figure 10. It allows NMR and ultrasonic measurements to be conducted together at different temperature and pressure conditions [76].
3. Teledyne ISCO Series D single-pump system. It is used to inject oil and brine into the cores.
4. Core lab recirculation pump system for confining fluid circulation and pressure control.
5. Pressure transducers and digital acquisition system to monitor and record pressure.
6. Square wave pulser-receiver and digital oscilloscope for pulse-echo ultrasonic measurements.
7. Vacuum pump to remove air from the system.
8. High-pressure valves to control the flow and pressure of the fluids.
9. Volumetric cylinders to collect the produce fluids.

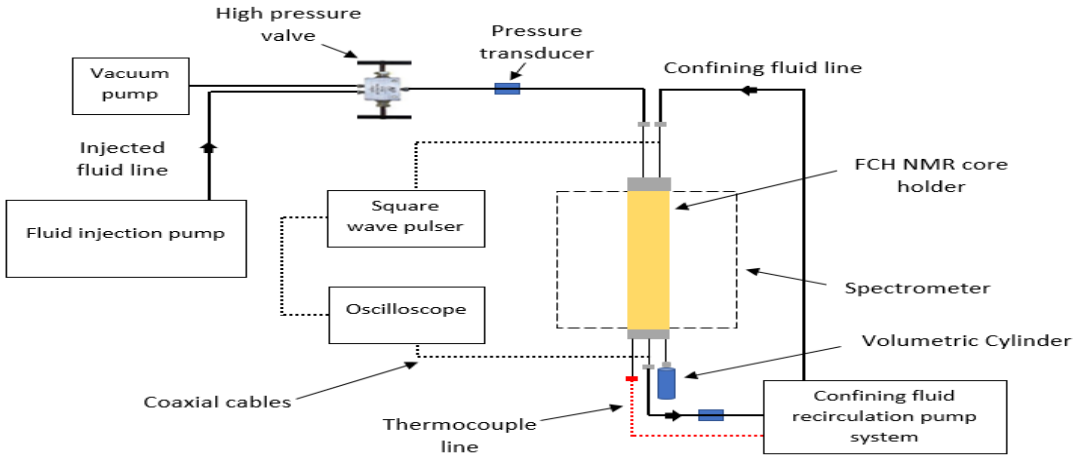

Figure 9 Experimental setup

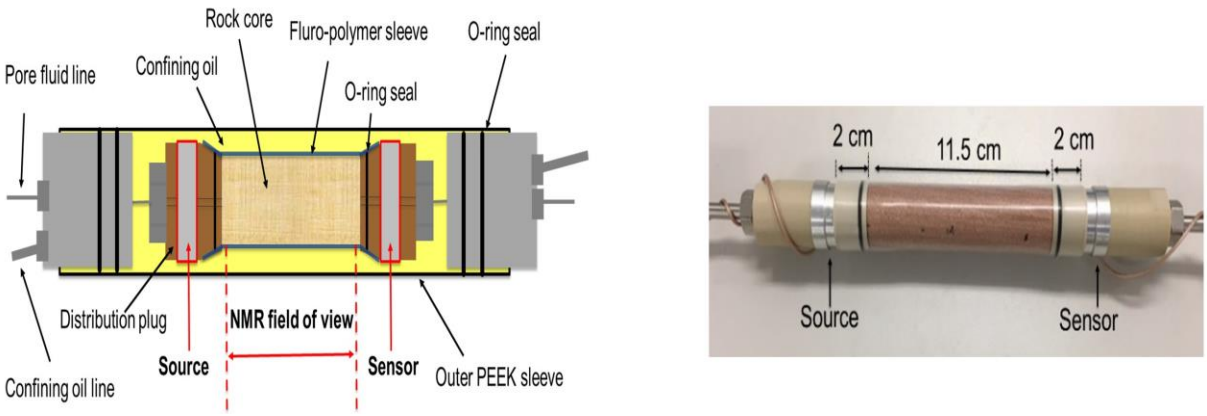

Figure 10 Modified FCH NMR comparable core holder [76]

3.1.2 Methodology

Firstly, rocks length, diameter, and porosity were determined. Porosity was measured by liquid saturation method [77]. Untreated Rocks properties are shown in Table 2. T_2 & T_1T_2 NMR measurements were conducted on the bulk fluids (paraffin oil and brine).

Table 2 Untreated rock properties

Sample	Dry weight (g)	Length (cm)	Diameter (cm)	Porosity (%)
SD	137.53	11.452	2.521	13
EB	110.71	11.452	2.521	29.1

The following procedure was conducted for both samples SD and EB:

1. Core sample that is originally water wet was dried and cleaned. The sample was placed in the core holder as shown in Figure 10. Then the core holder was put in the system showed in Figure 9.
2. The system was vacuumed.
3. NMR (T_2 & T_1T_2) and ultrasonic velocity measurements were conducted on the dry core. The reason for conducting NMR tests on the dry core is to identify the background noise produced by the system components so it is subtracted later on and not interpreted as a part of the signal.
4. Brine was injected into the sample until $S_w = 1$.
5. Brine was flooded into the fully saturated core and the permeability was measured.
6. NMR (T_2 & T_1T_2) and ultrasonic velocity measurements were conducted on the fully water saturated core.
7. Paraffin oil was injected into the core until a known value of S_w is reached.
8. NMR (T_2 & T_1T_2) and ultrasonic velocity measurements were conducted on the oil/water saturated core.

9. Core sample was cleaned and dried. Then, it was treated with (HTS) chemical to alter its wettability to oil wet. Silurian dolomite sample was saturated with pure HTS while Edward Brown carbonate was saturated with oil-in-water emulsion consisting of 5% by volume HTS and 95% deionized water. In addition, 300 ppm of surfactant (Span 80) was added to stabilize the emulsion in EB sample.
10. Steps 1 – 8 were repeated with the exception that the cores are now oil wet.

3.2 Second Approach: Wettability Alteration by Aging with Crude Oil

This approach is based on aging process at high temperature with oil that contains asphaltene to alter the wettability of rocks and conducting T_2 and T_1T_2 NMR measurements on the aged and non-aged samples at different saturations to evaluate rocks wettability. Detailed explanation of materials and methods used in this approach is provided below.

3.2.1 Materials and Equipment

Two Indiana limestone rock samples (1H, 2H) and two Berea sandstone samples named 1S, and 2S were cut form 12 in length cores as the one shown in Figure 11. Before Berea samples were used in this study, they were fired at 900 ^{o}C for 8 hours to stabilize or desensitize the clays [78] and rendered Berea strongly water-wet [79]. Samples porosity and permeability were determined using the AP-608 Automated Permeameter-Porosimeter, shown in Figure 12. Rock composition was identified using the PANalytical Empyrean Multi-Function XRD shown in Figure 13.

Figure 11 Indiana limestone rock core form which smaller samples are obtained for the study

Figure 12 AP-608 Automated Permeameter-Porosimeter

Figure 13 PANalytical Empyrean Multi-Function XRD

8 % NaCl brine and crude oil from the middle east are the fluids used in this study. The fluid density and viscosity measurements were conducted with hydrometer and Oswald viscometer and a temperature-controlled oil bath. ASTM D2007-80 standard procedure was followed for asphaltene content analysis except that n-heptane was used instead of n-pentane.

The URC-628 Ultra Rock Centrifuge, shown in Figure 14 was used for imbibition/drainage cycle. It consist of a data acquisition system. The rotor speed ranges from 1000 – 20,000 RPM.

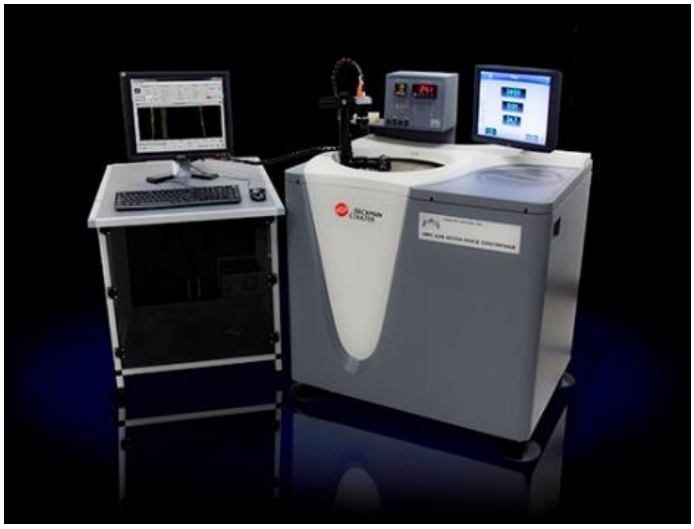

Figure 14 The URC-628 Ultra Rock Centrifuge

Figure 15 shows the Oxford Instruments' Geospec2-75, operating at 2.2 MHz used for NMR measurements. The NMR experiments were conducted at room temperatures and pressure. CPMG [50], [51] pulse sequence was used for T_2 measurements with signal to noise ratio above 100 and tau time of 0.05 ms ($T_{E,s}$ = 0.1 ms).

Figure 15 Oxford Instruments' Geospec2-75

3.2.2 Methodology

Firstly, brine was prepared by adding NaCl salt to deionized water and mixing for 30 minutes. Crude oil was obtained and filtered to remove any solid particles and impurities. Oil 1 has an API gravity of 26.12 and 5.67 wt% asphaltene. Oil 2 is taken from oil 1 but 1 wt% of asphaltene was added, so oil 2 has 6.67 wt.% asphaltene and 25.76 API gravity. Oil 1 was used for samples 1H, and 1S while oil 2 was used for 2H and 2S. The density and viscosity of the brine and oil were measured at different temperatures as shown in Figure 16 and Figure 17, respectively. Table 3 shows the fluids viscosity and density at 25 ^{o}C and 1 atm.

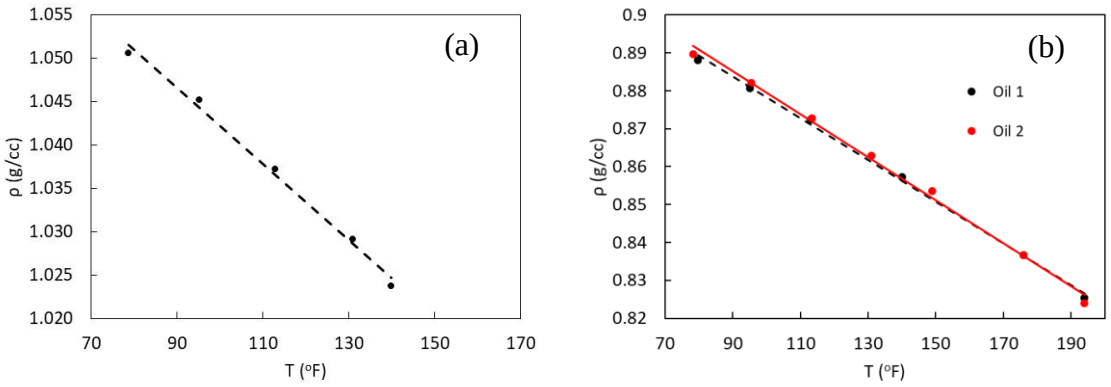

Figure 16 Measured density at different temperatures of brine (a), and oil (b)

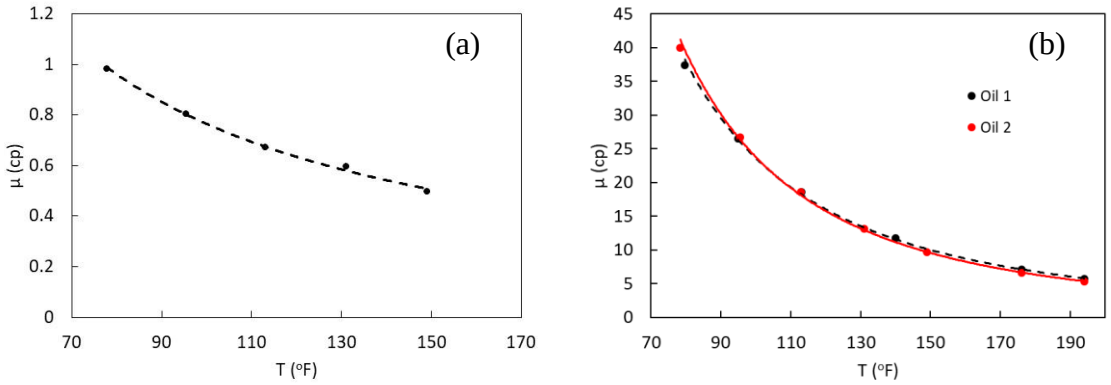

Figure 17 Measured viscosity at different temperatures of brine (a), and oil (b)

Table 3 Oil and brine density and viscosity at 25 ºC and 1 atm

Sample	Density (g/cc)	Viscosity (cp)
Brine	1.052	1
Oil 1	0.889	41
Oil 2	0.891	43

Table 4 presents rock samples properties. Rock mineral composition is shown in Figure 18.

Table 4 Rock sample properties

Sample	Diameter (cm)	Length (cm)	φ (%)	K (md)
1H	3.797	4.631	18.86	281.3
2H	3.804	4.907	18.54	274.2
1S	3.788	5.194	22.05	189.8
2S	3.789	5.172	21.61	157.5

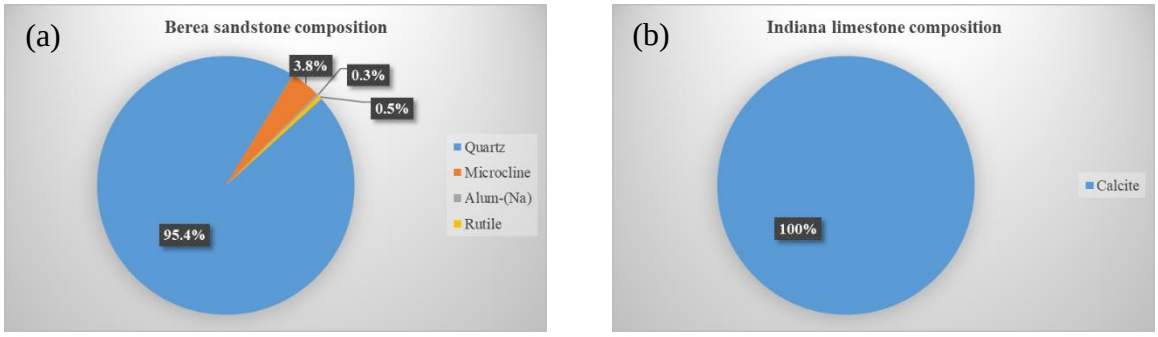

Figure 18 Mineral composition of Berea (a) and Indiana (b) rock samples

At the beginning, core samples were fully saturated with brine and T_2 and T_1T_2 NMR measurements were conducted at (S_w = 1). NMR measurements on bulk fluid were also conducted. Then, oil was injected into the samples (primary drainage) using URC-628 Ultra Rock Centrifuge until irreducible water saturation was reached and NMR measurements were run at (S_{wi}). Next, Indiana limestone samples were aged at 500 psi and 90 ^oC for one week to restore wettability towards a more oil-wet condition. Berea sandstone were not aged to ensure that they are water wet as known from earlier studies. The main reason for this step is to ensure that T_2 measurements can identify different wettability systems. NMR measurements were conducted on the aged Indiana limestone samples at S_{wi}. After that, brine was injected into the samples (imbibition) until residual oil saturation was achieved and NMR measurements were run at (S_{or}). After completing the previous work, oil 1 and oil 2 were injected again (secondary drainage) into the Indiana limestone samples 1H and 2H, respectively until S_{wi} is reached and NMR measurements were conducted. Then, the rock samples were aged again at 500 psi and 90 ^oC for 112 days and NMR measurements were conducted on sample 1H and 2H.

CHAPTER 4

RESULTS AND DISCUSSION

This section explained the obtained results. The observations and results are discussed in details.

4.1 First Approach: Wettability Alteration by Chemical Treatment

Figure 19 shows the fluids hydrogen index. We see that brine hydrogen index (0.92) is less than that of paraffin oil (1.2). Due to difference in H-index, the oil peak is much higher than the water peak so we plotted the normalized T_2 distribution in Figure 20 to have comparable amplitude for convenient comparison. There is a clear separation between the oil and water T_2 peaks because of contrast between their viscosities. T_2 of bulk brine is 2.32 seconds while T_2 of paraffin oil is 0.024 seconds. T_1T_2 maps of the bulk brine and oil are presented in Figure 21 (a) and (b), respectively. Both paraffin oil and brine have T_1/T_2 ratio equal to 1 which is usually the expected behavior for bulk fluids.

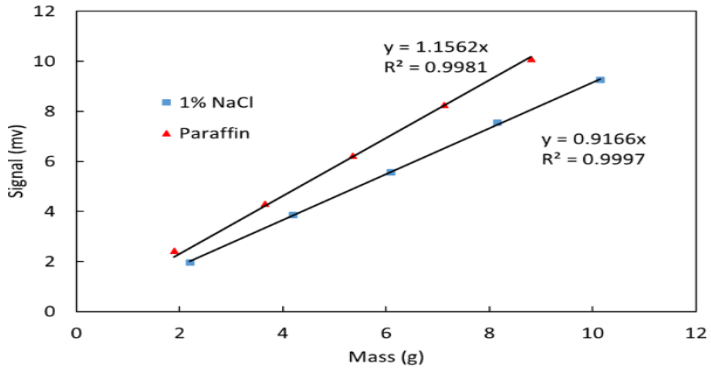

Figure 19 Hydrogen index of the fluids

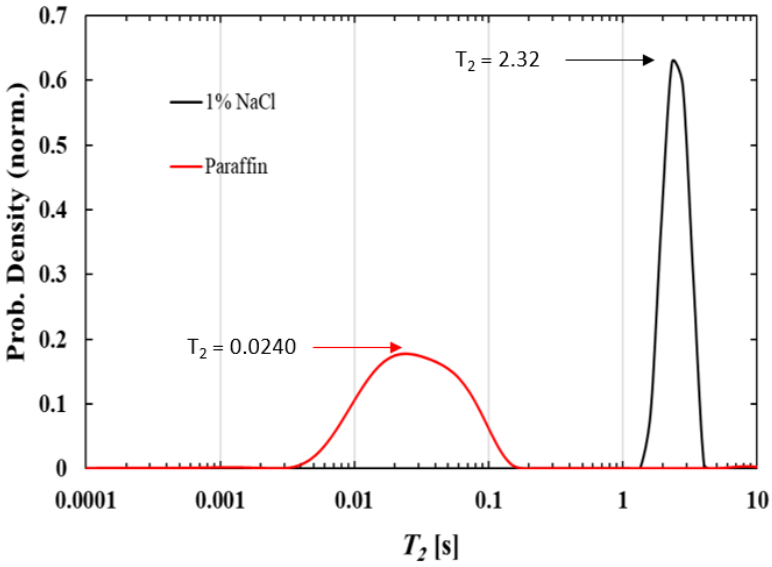

Figure 20 Fluids T_2 distribution

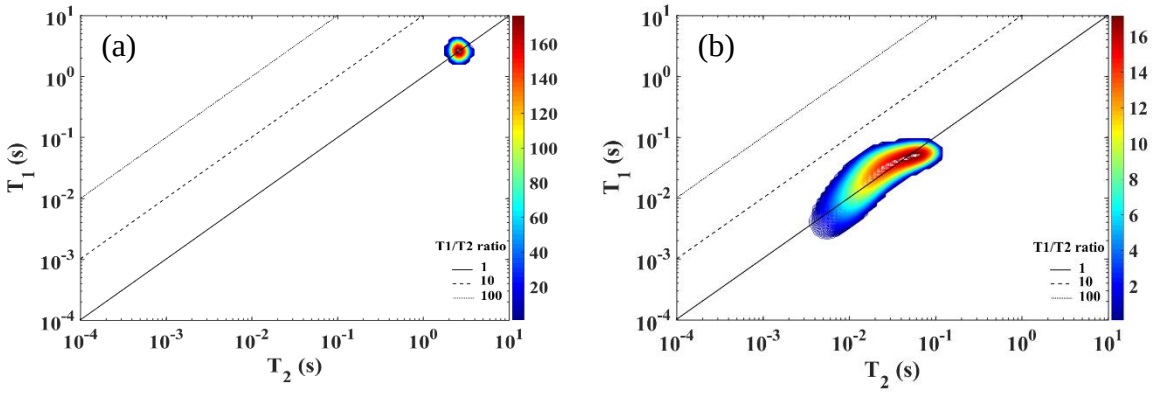

Figure 21 T_1T_2 maps of brine (a) and paraffin oil (b)

As mentioned in the methodology that NMR measurements were conducted on the dry core to find the background signal produced from the system components and subtracted from the results when the core is saturated so we are sure that the produced signal is only from the fluids inside the pore space. To illustrate this, Figure 22 is provided below as an example. We see that in Figure 22 (a), that part of the signal with very low probability density is spread along the T_1T_2 map but it seems unrealistic and it is attributed to the background signal. The noise signal was removed by subtracting the row T_1T_2 data obtained from the measurement on the treated

dry SD core from the row T_1T_2 data obtained from the measurement on the treated saturated SD core and then Figure 22 (b) was generated.

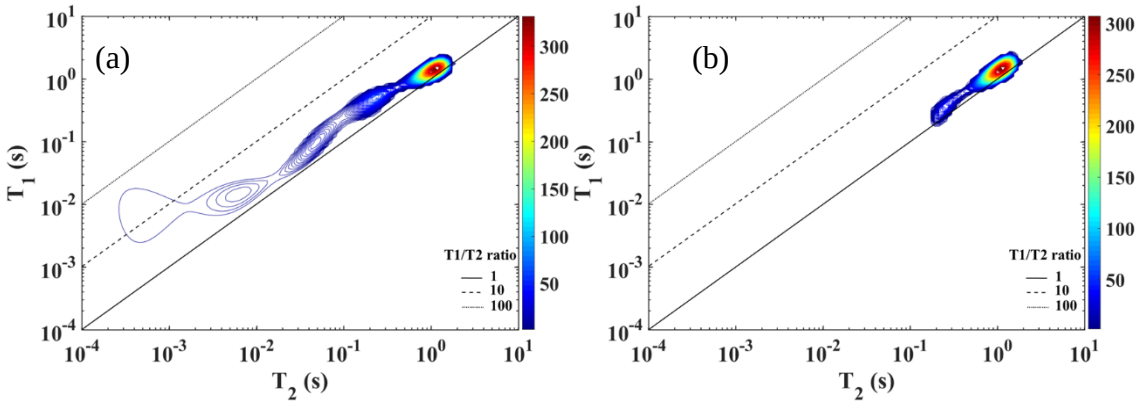

Figure 22 Background removal example (Treated SD sample that is fully saturated with brine)

4.1.1 Measurements on Silurian Dolomite Sample

After saturating the core fully with brine, the brine was injected at different rates to determine the permeability of the untreated sample. It was determined to be 31.5 md as shown in Figure 23.

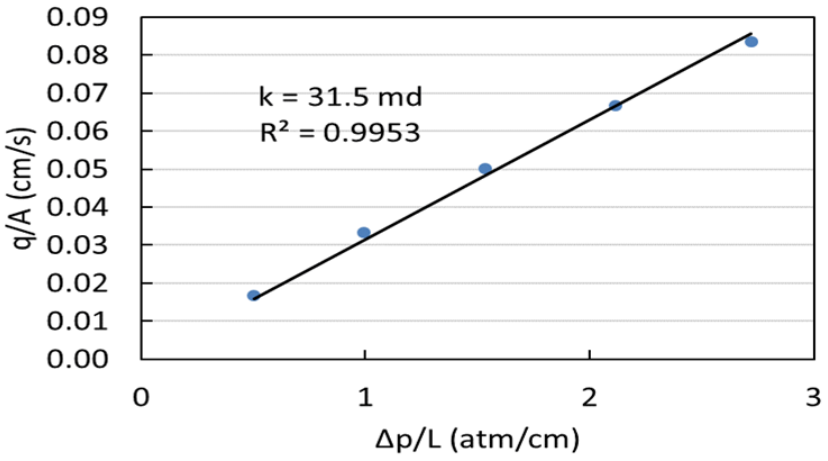

Figure 23 Untreated SD core flooding experiment

T_2 distribution of untreated SD at S_w= 1 and after injection paraffin are shown in Figure 24. T_2 distribution of a fully water saturated sample is directly related to its pore size distribution. We see that the sample consist of dual pore system since there are two peaks when the sample is fully brine saturated. In addition, the macrospores are the dominant pores compared to the microspores since their corresponding peak is higher than that of microspores. Furthermore, the two pore systems are well connected as appears clearly in the fully water saturation T_2 distribution (Figure 24). Oil was injected until S_w = 0.56 but it is difficult to infer wettability from T_2 distribution of brine/paraffin saturated rock without the separation of oil and water signals so T_2-D measurements would help in this case.

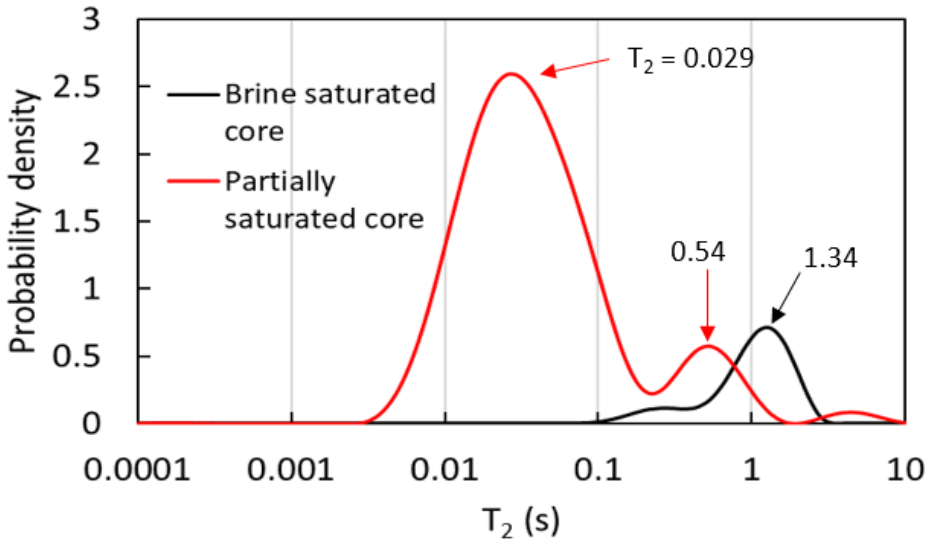

Figure 24 T_2 distribution at fully and partially brine saturated untreated SD sample

T_1T_2 maps of untreated SD at S_w=1 and after injection paraffin are shown in Figure 25 (a) and (b), respectively. We can clearly see the surface relaxation effect when the core was fully saturated with brine (Figure 25 (a)) such that T_1/T_2 ratio was shifted above the unity line compared to the bulk brine T_1/T_2 ratio (Figure 21 (a)). After injection paraffin (Figure 25 (b)),

two peaks appeared. The T_1/T_2 ratio of paraffin oil inside the rock (left peak in Figure 25 (b)) was on the unity line close to its bulk T_1/T_2 ratio (Figure 21 (b)) so the rock is water wet. This can be confirmed by comparing the T_1/T_2 ratio of bulk brine (Figure 21 (a)) and brine inside the rock (right peak in Figure 25 (b)). Bulk brine $T_1/T_2 = 1$ while inside the rock, it shows T_1/T_2 ratio of 1.26.

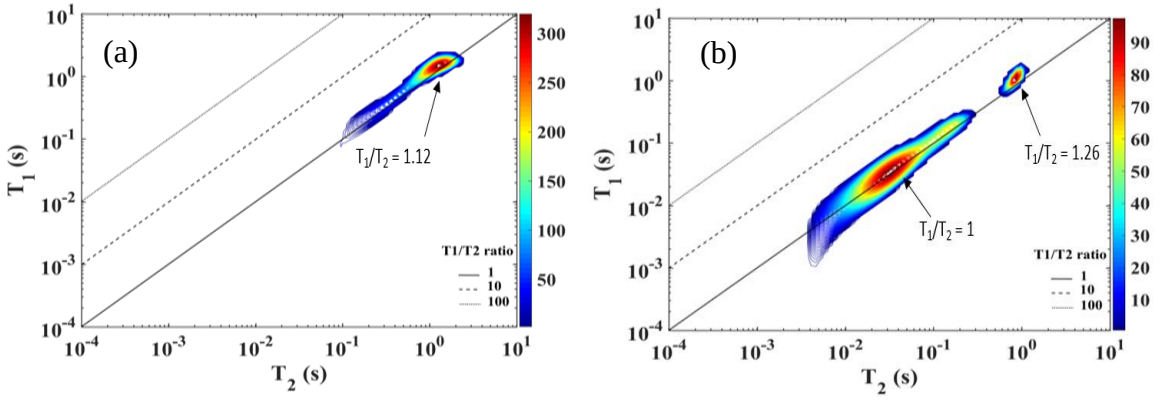

Figure 25 T_1T_2 maps of untreated SD at fully brine saturated (a) and partially saturated (b)

After the untreated SD sample was cleaned and dried, it was treated by saturating it with 100% HTS chemical. Then, the treated core was cleaned and dried again to be used again. The permeability of the treated oil wet sample was reduced dramatically to 6.7 md as shown in Figure 26. The reason for this reduction is that the concentration of the treating chemical was very high causing it to react and dissolve the rock surface and plugging the pore throats. The paraffin injection pressure at q = 0.5 ml/min was monitored before and after the treatment. It was observed how the injection pressure, after treatment Figure 27 (b), increases significantly compared to that before treatment, Figure 27 (b). The increase in pressure is attributed to the significant permeability reduction.

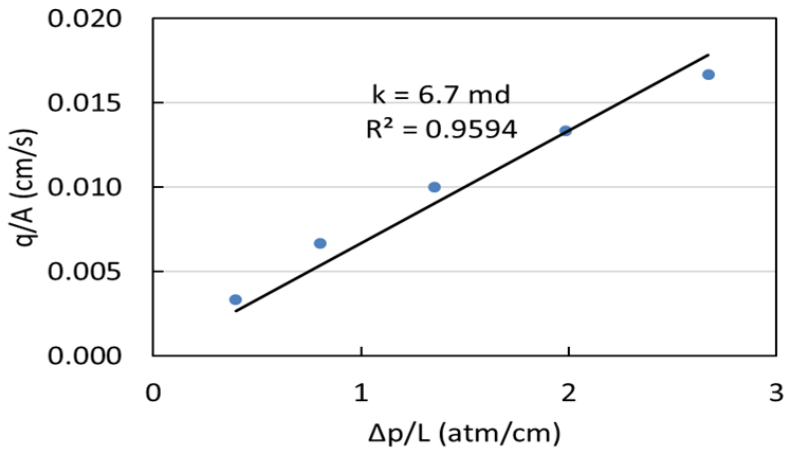

Figure 26 Treated SD core flooding experiment

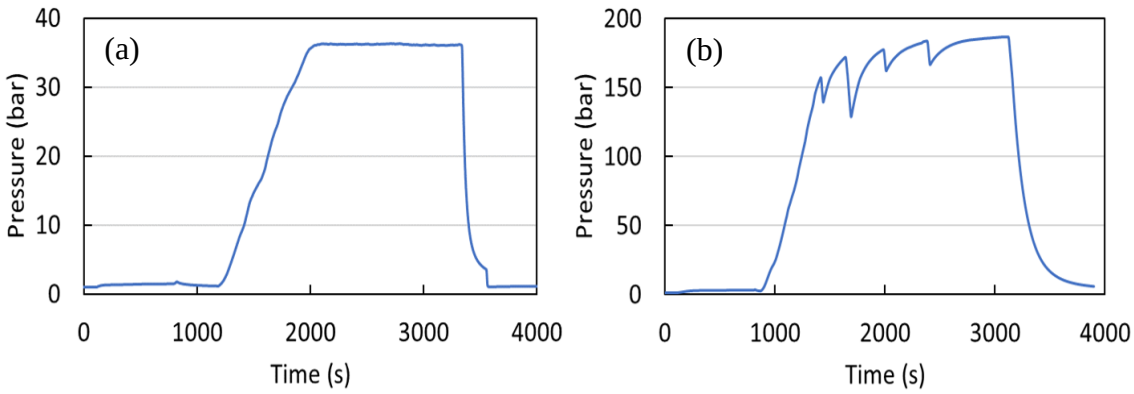

Figure 27 Paraffin injection pressure with time for untreated SD (a), and treated SD sample (b)

T_2 distribution of the treated SD sample at S_w = 1 and after injection paraffin are shown in Figure 28. We see that the sample still consist of dual pore system since there is two T_2 peaks (0.93 s, and 0.18 s) when the sample is fully brine saturated. However, the connectivity between the two pore systems is significantly reduced to the permeability reduction which appears clearly in the fully water saturation T_2 distribution (Figure 28). Paraffin was injected with the same rate of that before the treatment as shown in Figure 27 (a) and (b) but the final water saturation achieved was S_w = 0.2 in this case and it is much more smaller than that before the treatment which indicates that the rock became oil wet. However, it is still difficult to infer

wettability from T_2 distribution of brine/paraffin saturated rock without the separation of oil and water signals.

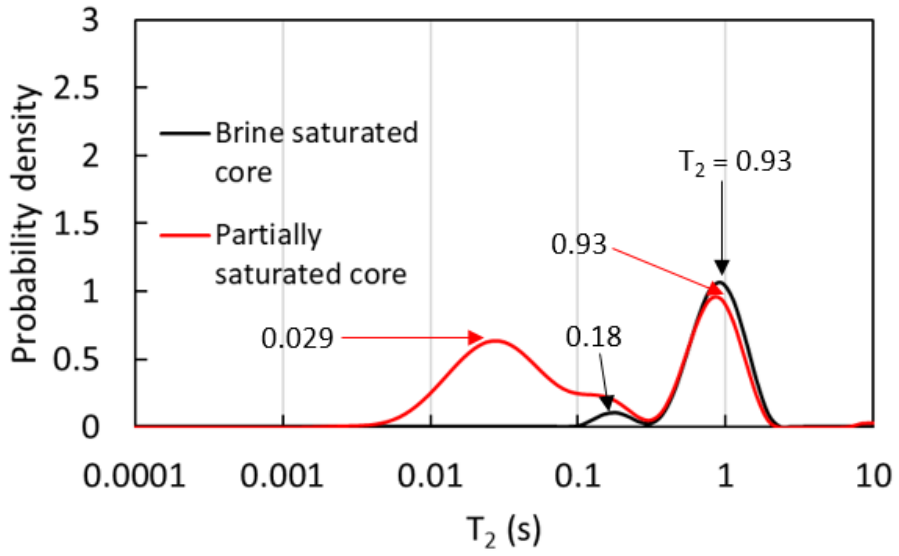

Figure 28 T_2 distribution at fully and partially brine saturated treated SD sample

T_1T_2 maps of treated SD at S_w= 1 and after paraffin injection are shown in Figure 29 (a) and (b), respectively. In Figure 29 (b), oil and water signals overlap making wettability interpretation challenging so T_2-D measurements are needed to separate the oil and water signals.

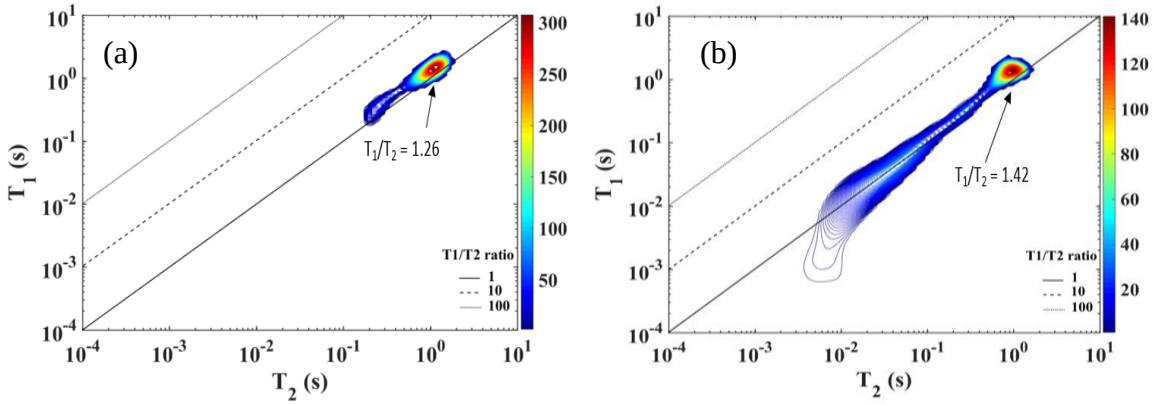

Figure 29 T_1T_2 maps of treated SD at fully brine saturated (a) and partially saturated (b)

Ultrasonic velocity measurements of untreated SD, and treated SD at different conditions are shown in Figure 30 (a) and (b), respectively. An example of P-wave arrival time at effective stress = 55 bar for untreated SD, and treated SD at different conditions is shown in Figure 31 (a) and (b), respectively.

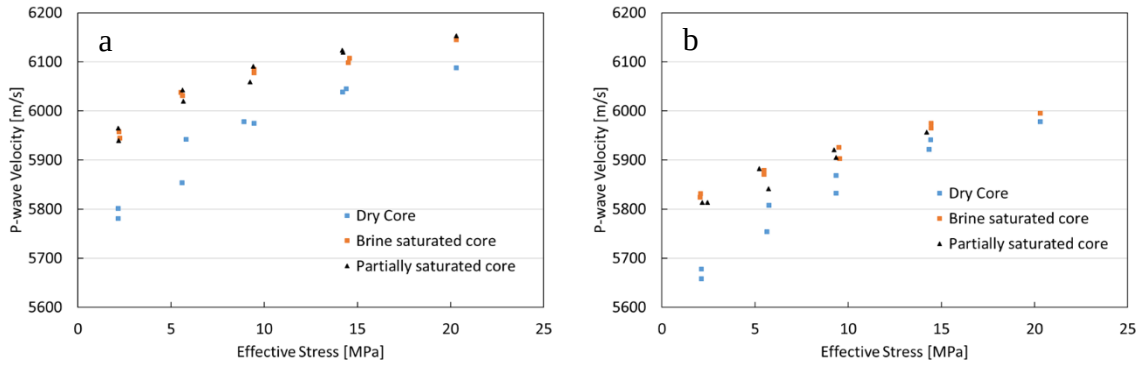

Figure 30 Ultrasonic velocity measurements of untreated SD (a), and treated SD (b) at different conditions

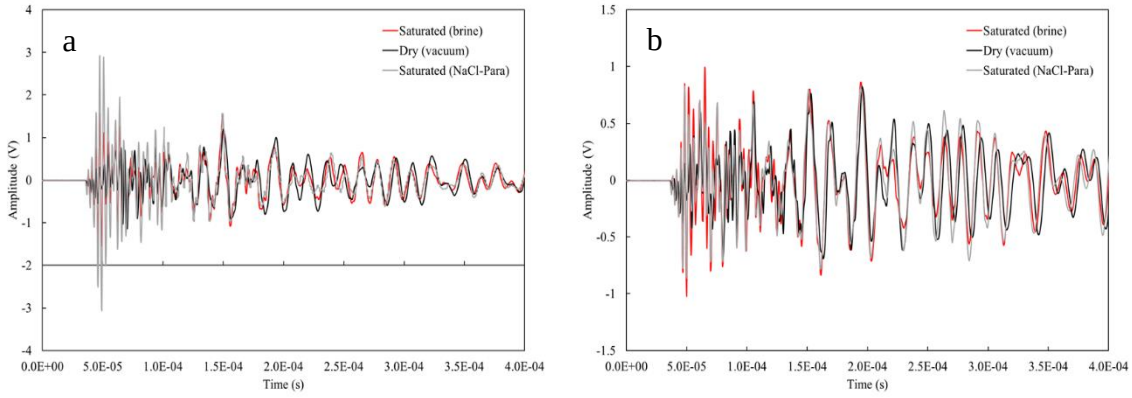

Figure 31 P-wave arrival time at effective stress = 55 bar of untreated SD (a), and treated SD (b) at different conditions

4.1.2 Measurements on Edward-Brown Carbonate Sample

At the beginning, permeability of the untreated originally water wet sample was determined to be 28.4 md by core flooding as shown in Figure 32.

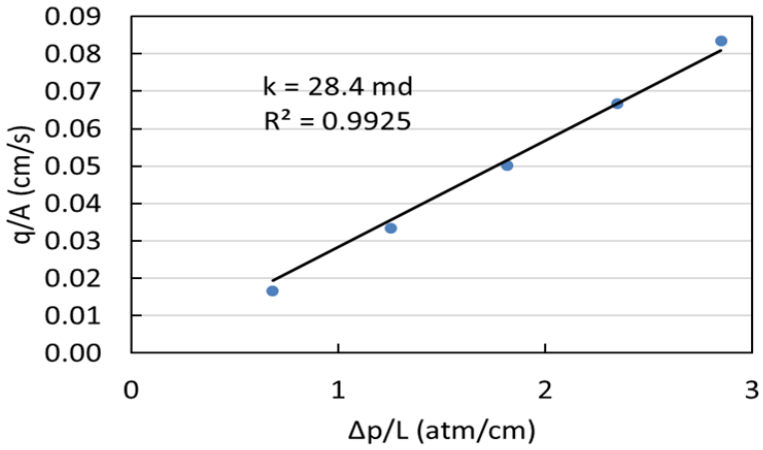

Figure 32 Untreated EB core flooding results

T_2 distribution of untreated EB at S_w=1 and after paraffin injection are shown in Figure 33. We see that the sample consist of dual pore system since there are two peaks when the sample is fully brine saturated. In addition, the macrospores are the dominant pores compared to the microspores since their corresponding peak is higher than that of microspores. Furthermore, the two pore systems are well connected as appears clearly in the fully water saturation T_2 distribution. When Oil was injected until S_w = 0.76, only one peak appeared and this could be attributed to the pore coupling effect in carbonate rocks. In addition, it is difficult to infer wettability from T_2 distribution of brine/paraffin saturated rock without the separation of oil and water signals so T_2-D measurements would help in this case.

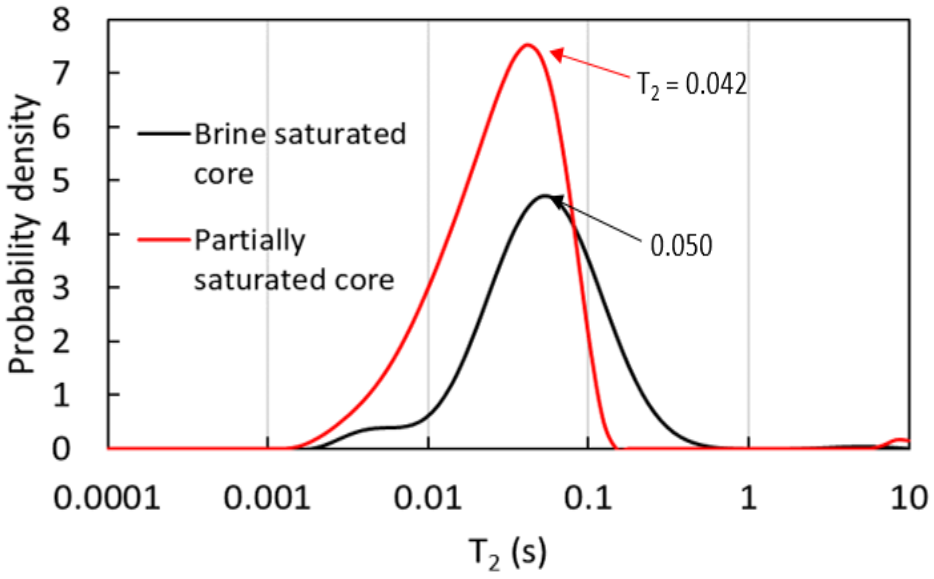

Figure 33 T_2 distribution at fully and partially brine saturated untreated EB sample

T_1T_2 maps of untreated EB at S_w=1 and after paraffin injection are shown in Figure 34 (a) and (b), respectively. Oil and water signals overlap making wettability interpretation from T_1T_2 maps challenging so T_2-D measurements are needed to separate the oil and water signals.

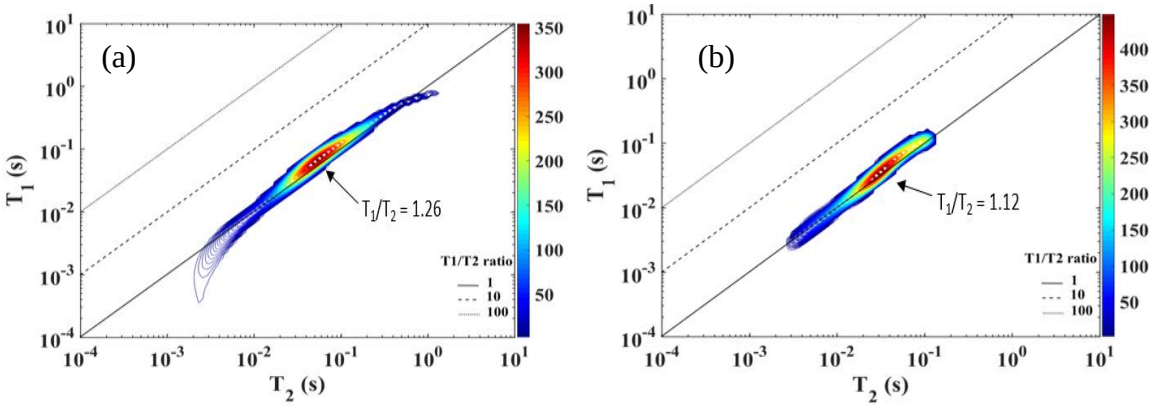

Figure 34 T_1T_2 maps of untreated EB at fully brine saturated (a) and partially saturated (b)

After the untreated EB sample was cleaned and dried, it was treated by saturating it with oil-in-water emulsion consisting of 5% by volume HTS and 95% deionized water in addition to 300 ppm of surfactant (Span 80) to stabilize the emulsion. The main reason for reducing the concentration of the treatment chemical is to avoid its interaction with rock as occurred in SD sample. Then, the treated core was cleaned and dried again. The permeability of the treated oil wet sample was 31.8 md as shown in Figure 35, which is almost the same as that of untreated sample. The paraffin injection pressure at q = 0.5 ml/min was monitored before and after the treatment. Same injection pressure was recorded before and after the treatment as shown Figure 36 (a) and (b), respectively. Figure 37 shows a droplet of water on EB sample after treatment with HTS. It is clear how it becomes oil wet.

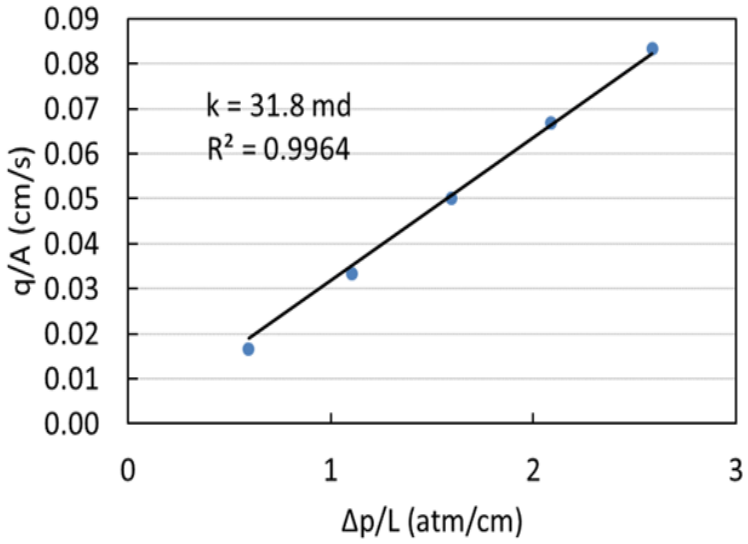

Figure 35 Treated EB core flooding results

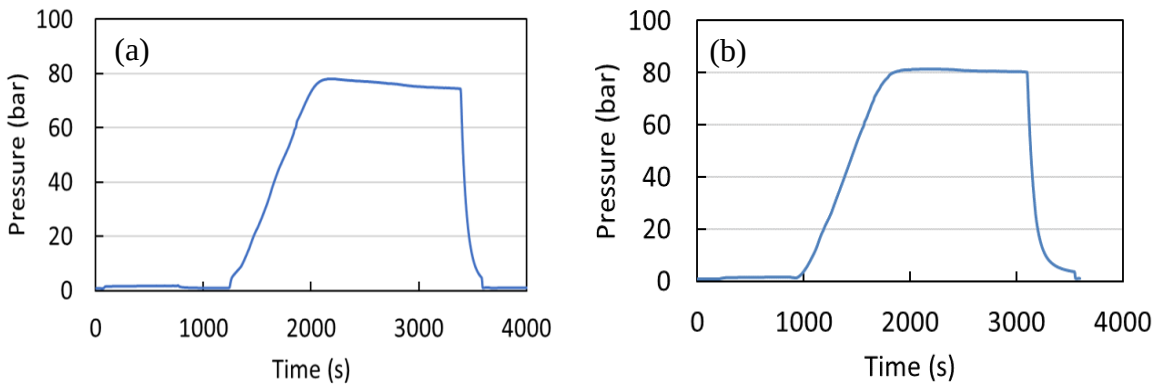

Figure 36 Paraffin injection pressure with time for untreated EB (a), and treated EB sample (b)

Figure 37 Droplet of water on EB sample after treatment with HTS. It is clear how it becomes oil wet

T_2 distribution of the treated EB sample at $S_w = 1$ and after injection paraffin are shown in Figure 38. We can see that the T_2 distribution after treatment is very similar to that before the treatment. We can conclude that our treatment method was not well conducted such that when the brine was injected for permeability measurements, the chemical was flushed out of the core. To improve the treating method, aging time at high temperature is required to allow the chemical to be adsorbed in the rock surface and alter its wettability permanently.

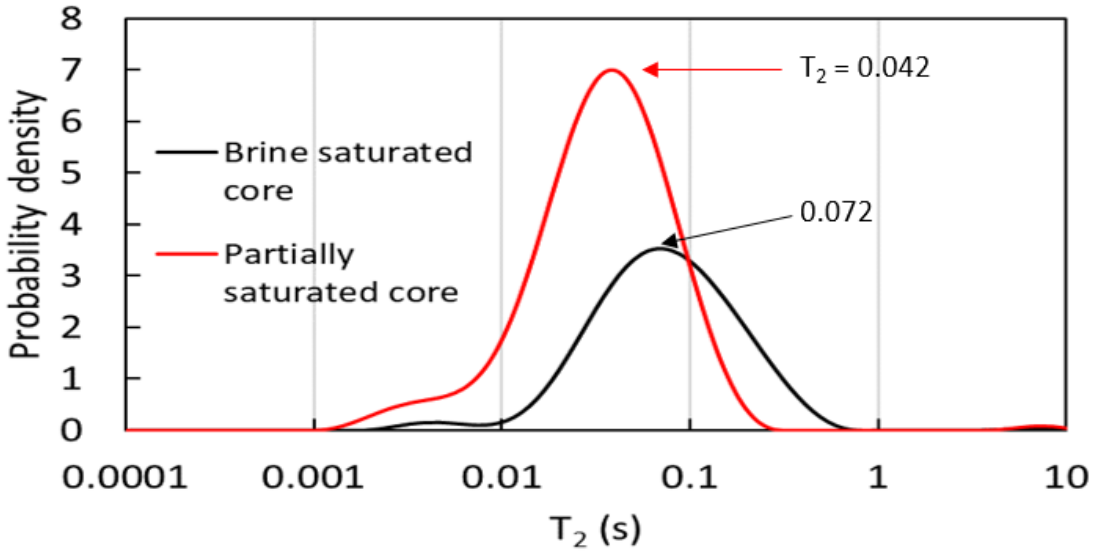

Figure 38 T_2 distribution at fully and partially brine saturated treated EB sample

T_1T_2 maps of treated EB at S_w=1 and after paraffin injection are shown in Figure 39 (a) and (b), respectively. They are also very similar to that before treatment and the same conclusion obtained from T_2 distributions applies here that the rock treatments failed and appropriate chemical concentration and aging time should be chosen to alter the rock wettability.

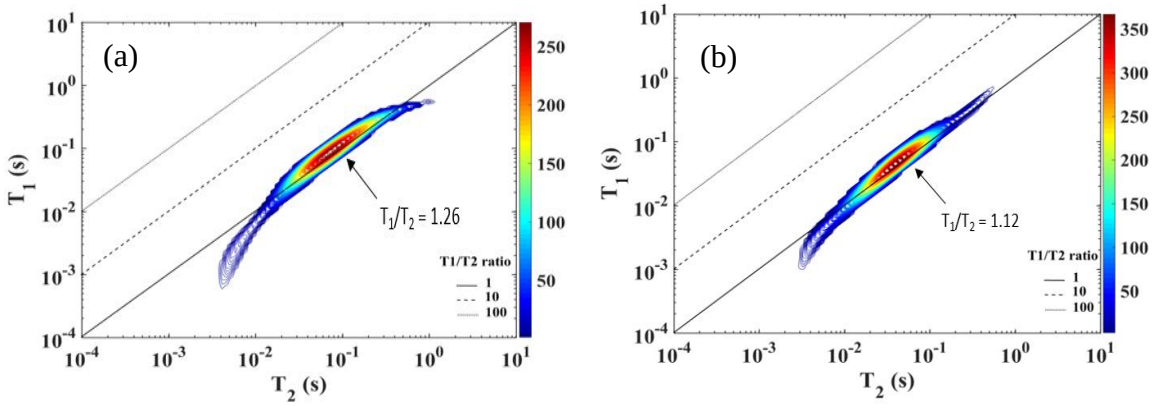

Figure 39 T_1T_2 maps of treated EB at fully brine saturated (a) and partially saturated (b)

Ultrasonic velocity measurements of untreated EB, and treated EB at different conditions are shown in Figure 40 (a) and (b), respectively. An example of P-wave arrival time at effective stress = 55 bar for untreated EB, and treated EB at different conditions is shown in Figure 41 (a) and (b), respectively.

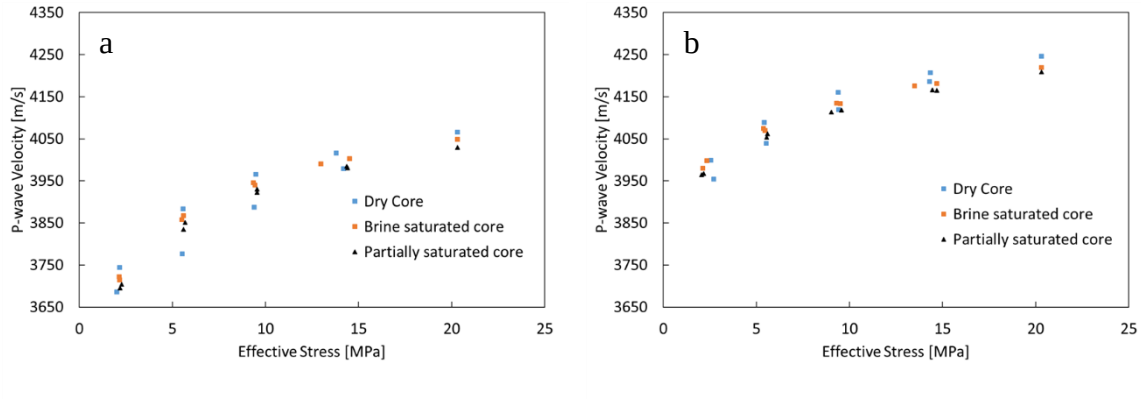

Figure 40 Ultrasonic velocity measurements of untreated EB (a), and treated EB (b) at different conditions

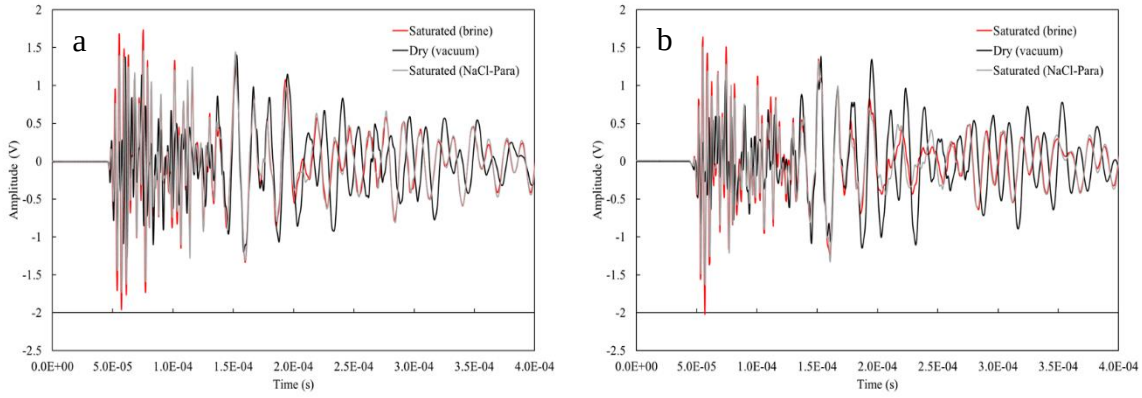

Figure 41 P-wave arrival time at effective stress = 55 bar of untreated EB (a), and treated EB (b) at different conditions

4.2 Second Approach: Wettability Alteration by Aging with Crude Oil

4.2.1 T_2 Measurements

Figure 42 presents T_2 distribution for the bulk oils and water. There is a clear separation between the oil and water T_2 peaks because of the significant contrast between their viscosities as shown in Table 3. T_2 of bulk brine is 2.78 seconds while the two oils has the same predominant peak at T_2 = 0.0864 seconds and the smaller peak is at 0.005572 seconds. The reason that oil has two peaks is attributed to the variation in the crude oil composition from light to heavy components which is the expected behavior [58], [80] . The oil peak is much higher than the water peak so we plotted the normalized amplitude in Figure 42 to make it more convenient.

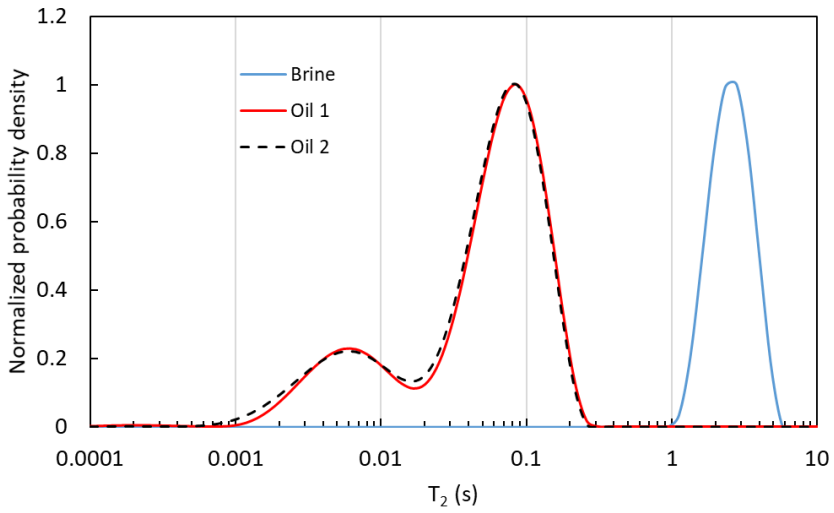

Figure 42 T_2 distribution of bulk fluids

T_2 distribution of sample 1H fully saturated with brine is shown in Figure 43 (a). Since brine is the only phase inside the pore space, it exhibits surface relaxation and we can see that the

predominant peak T_2 has been shifted to the left compared to the bulk water T_2 represented by the black dotted line. Furthermore, for fully water-saturated sample, T_2 predicts the pore size distribution and we see that we have two connected pore systems (macro and micro). When oil 1 is injected until S_{wi}, the larger pores were filled first by oil, while irreducible water saturation remains in the smaller pores. From Figure 43 (b), we see that the predominant peak T_2 was shifted to the exact bulk oil T_2 represented by the red dotted line which indicates that the sample is originally strong water wet and oil is not the wetting phase so it does not show any surface relaxation effect. Once the rock was aged for one week, the wettability condition starts to change and this is clearly indicated by the shift of the predominant peak T_2 to 0.0599 s compared to 0.0864 s before aging as shown in Figure 43 (c). However, the shift is not that significant which indicates that the wettability is close to intermediate condition and more likely water wet. It is also observed that T_2 distribution at S_{wi} after aging, shows only single peak compared to that at S_{wi} before aging. This could be attributed to the enhancement of the pore coupling effect by organic material deposition and adsorption after aging [34], [81], [82]. Water was injected until S_{or} and Figure 43 (d) confirms that the wettability in the large pores is intermediate and more likely water wet since the predominant peak T_2 was shifted slightly to the right 0.93 s compared to the fully water saturated T_2 (0.373 s). This behavior indicates that surface relaxation effect on water was reduced since oil starts also to wet some of the large pore surfaces but water still coats most of the pore surface. We can confirm this by comparing T_2 after imbibition (0.93 s) to bulk water T_2 (2.78 s) and fully water saturated T_2 (0.373 s). We clearly see that T_2 after imbibition is still closer to T_2 of the fully water saturated case than to the bulk brine T_2. In addition, we see from Figure 43 (d) that after imbibition, the small pores are still saturated by

water only and hence they are water wet since we see that the smaller peak was shifted again to the same peak position for fully water saturated sample.

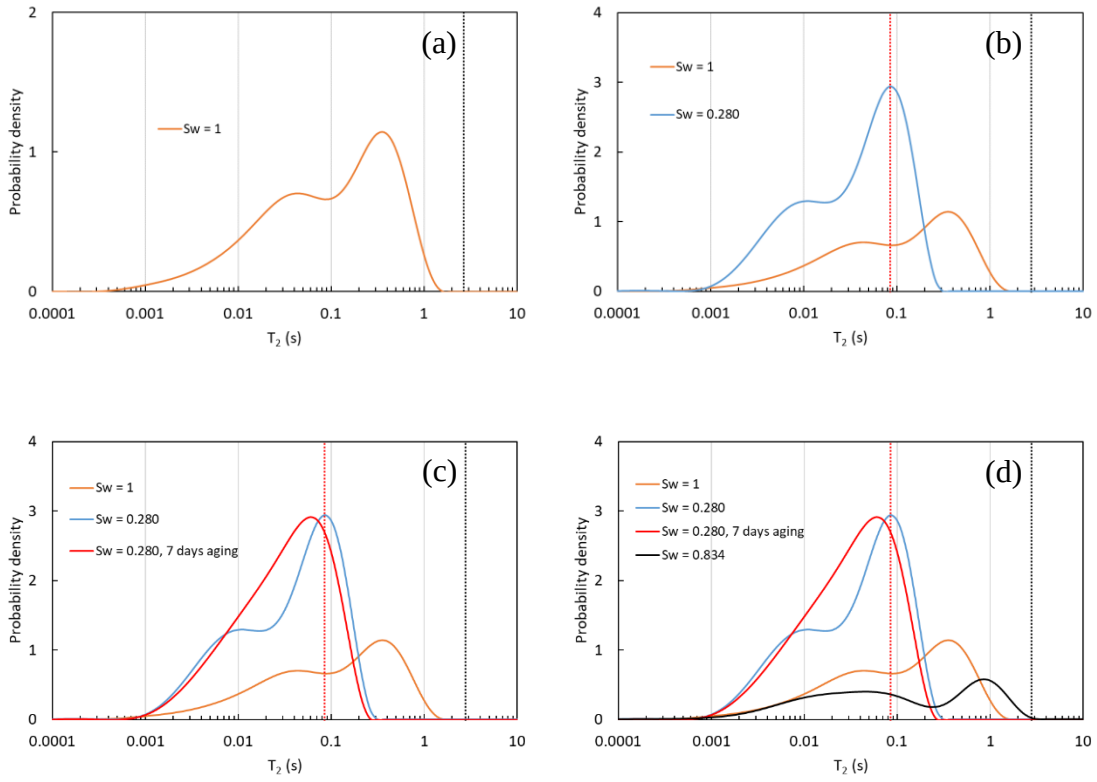

Figure 43 T_2 distribution of sample 1H at 100% brine saturated (a), after primary drainage (b), after aging (c), and after imbibition (d). The black dotted line represents the bulk brine T_2 while the red dotted line is the bulk oil 1 predominant peak T_2

Similar behavior was noticed in sample 2H. However, it is more likely to be less wetting to water compared to sample 1H due to the 1 wt% added asphaltene. The previous conclusion appears clearly in Figure 44 such that we see more shift to the left in T_2 after aging and more shift to the right in T_2 after imbibition compared to sample 1H. The predominant peak T_2 when fully brine saturated is 0.373 s, which is the same for sample 1H. When oil 2 was injected until S_{wi}, we see that the predominant peak T_2 was shifted to 0.072 s, which is almost the same as the bulk oil T_2 represented by the red dotted line, which indicates that the sample is originally water

wet and. After aging the sample for one week, the wettability was restored closer to the oil wet conditions and this is clearly indicated by the shift of the predominant peak T_2 to 0.0416 s compared to the bulk oil T_2 (0.0864 s) as shown in Figure 44. In addition, we clearly see that predominant peak T_2 after imbibition was shifted to 1.12 s due to the reduction of surface effect on the water phase. Nevertheless, the sample remains intermediate wet since the surface relaxation effect on water persists so that the T_2 is not very close to that of the bulk water. Finally, we see from Figure 44 that after imbibition the small pores are still saturated by water only and hence they are water wet since we see that the smaller peak was shifted again to the same peak position for fully water saturated sample.

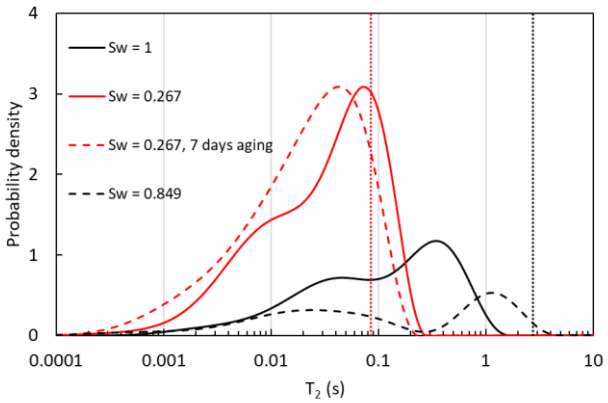

Figure 44 T_2 distribution of sample 2H at different saturations. The black dotted line represents the bulk brine T_2 while the red dotted line is the bulk oil predominant peak T_2.

Table 5 summarizes the predominant peak T_2 values after aging and after imbibition for Indiana limestone samples.

Table 5 Summary of the predominant peak T_2 values at different saturations for carbonate samples

Sample	$T_{2,Sw=1}$	$T_{2,Swi}$ (before aging)	$T_{2,Swi}$ (7 days aging)	$T_{2,Sor}$
1H	0.373	0.0864	0.0599	0.93
2H	0.373	0.072	0.0416	1.12

Figure 45 (a) presents T_2 distribution of sample 1S fully saturated with brine. We see that the predominant peak T_2 has been shifted to the left (0.149 s) compared to the bulk water T_2 represented by the black dotted line which indicates surface relaxation effect. When oil 1 is injected until $S_{wi,}$ Figure 45 (b), the predominant peak T_2 was shifted to 0.072 s that is almost the same as the bulk oil T_2 represented by the red dotted line, which indicates that oil is not the wetting phase so it does not shows any surface relaxation effect. In addition, T_2 distribution at S_{wi} is almost the same as the bulk oil distribution as shown in Figure 45 (b) which indicates that the sample is strongly water wet since oil behaves exactly like the bulk fluid although it is inside a pore space. Water was injected until S_{or} and Figure 45 (c) confirms that the rock is strongly water wet since the predominant peak T_2 was shifted to the exact value of T_2 when fully brine saturated (0.149 s) and T_2 distribution for the two cases is identical. Sample 2S shows the exact behavior of 1S as shown in Figure 46 although oil 2 was used for sample 2S. This indicates that the added 1 wt% of asphaltene makes no difference without aging.

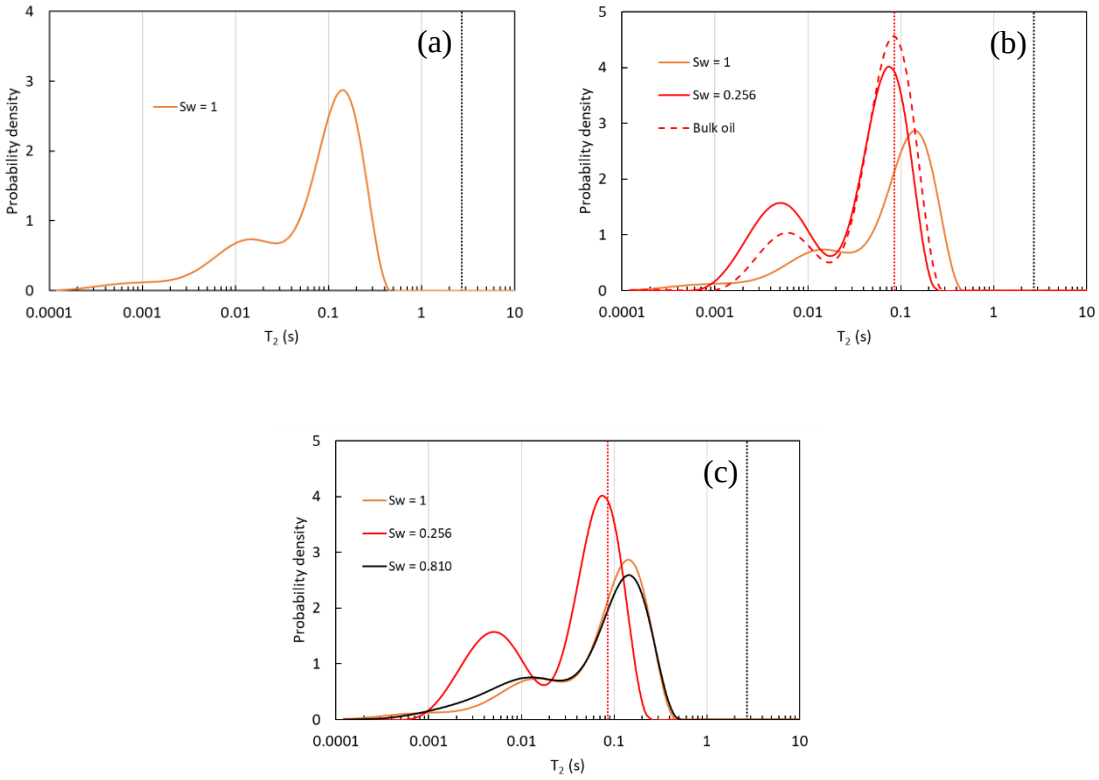

Figure 45 T_2 distribution of sample 1S at 100% brine saturated (a), after primary drainage (b), and after imbibition (c). The black dotted line represents the bulk brine T_2 while the red dotted line is the bulk oil predominant peak T_2

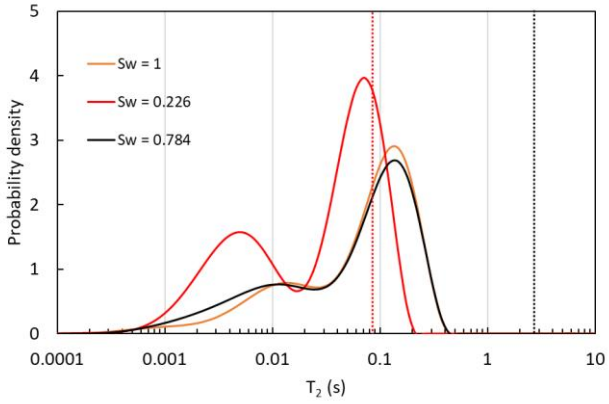

Figure 46 T_2 distribution of sample 2S at different saturations. The black dotted line represents the bulk brine T_2 while the red dotted line is the bulk oil predominant peak T_2

Table 6 summarizes the predominant peak T_2 values after primary drainage and after imbibition for Berea sandstone samples.

Table 6 Summary of the predominant peak T_2 values at different saturations for sandstone samples

Sample	$T_{2,Sw=1}$	$T_{2,Swi}$	$T_{2,Sor}$
1S	0.149	0.072	0.149
2S	0.149	0.072	0.149

NMR can be also used, as a quick tool to monitor wettability alteration especially when time is critical, which is usually the case in the oil field. After completing the above work, oil 1 and oil 2 were injected again (secondary drainage) into the Indiana limestone samples 1H and 2H, respectively until S_{wi} is reached and T_2 NMR measurements were conducted. Then, the rock samples were aged again at 500 psi and 90 ^{o}C for 112 days. From Figure 47, we see that after secondary drainage the T_2 values in both sample 1H and 2H are the same as that of primary drainage after aging, which is expected. However, after aging for 112 days, the peak were shifted to the left, which means that the surface relaxation effect is increasing on the oil phase and the rocks become more oil wet. The shift in T_2 distribution of sample 2H is greater than that of 1H due to the added asphaltene quantity. This means that aging time and asphaltente content are the main two factors controlling wettability alteration. This behavior agrees with the study conducted by Shikhov et al. [42]. The main idea here is to show how NMR is used to monitor wettability alteration or condition with time, which can save time and effort especially when applied in field by the mean of logging.

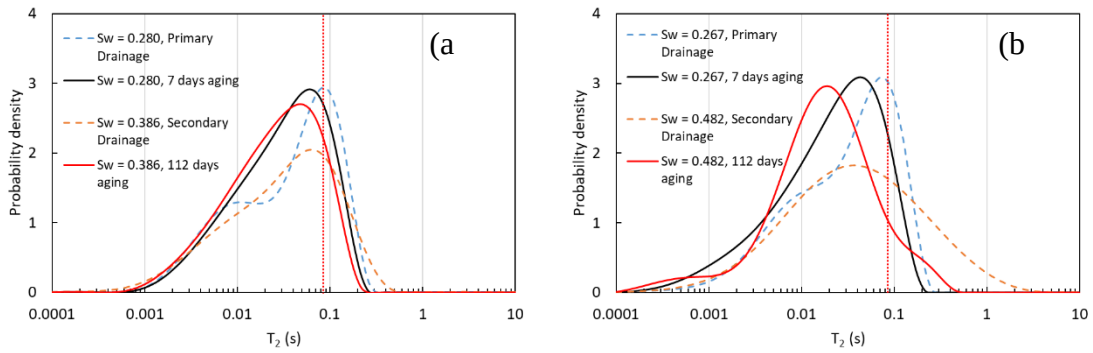

Figure 47 T_2 distribution of sample 1H (a), and 2H (b) at different conditions. The red dotted line is the bulk oil predominant peak T_2

4.2.2 T_1T_2 Measurements

T_1T_2 maps of brine, oil 1, and oil 2 are shown in Figure 48, Figure 49, and Figure 50, respectively. Table 7 presents T_1/T_2 ratio of bulk fluids. T_1/T_2 ratio of bulk brine locates on the unity line as expected. However, T_1/T_2 ratio of bulk oils deviates from unity due to intrinsic bulk oil properties [41]. Asphaltene presence in crude oil is the main reason of deviation from 1-1 line in T_1T_2 maps. If this deviation from unity were related to wettability, it would result in wrong conclusions.

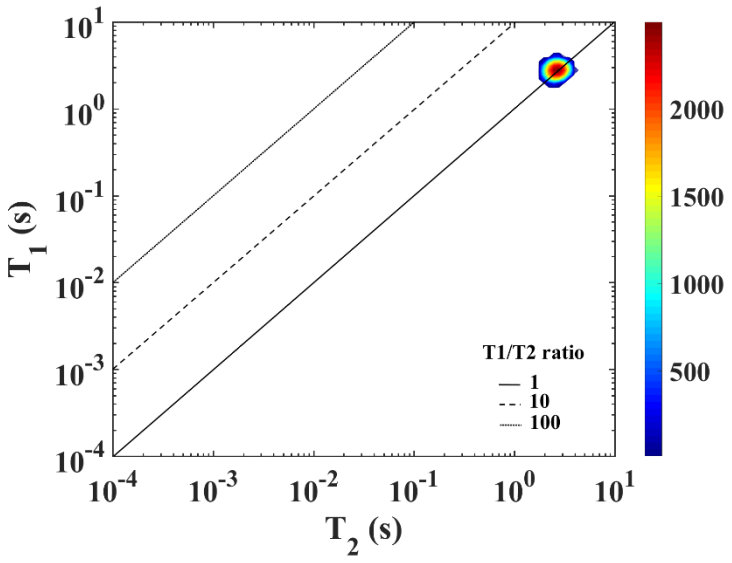

Figure 48 T_1T_2 map of bulk brine

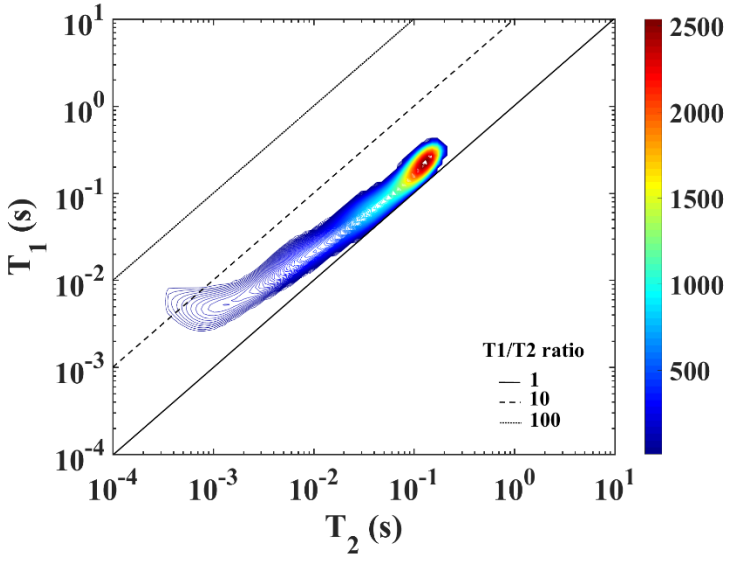

Figure 49 T_1T_2 map of bulk oil 1

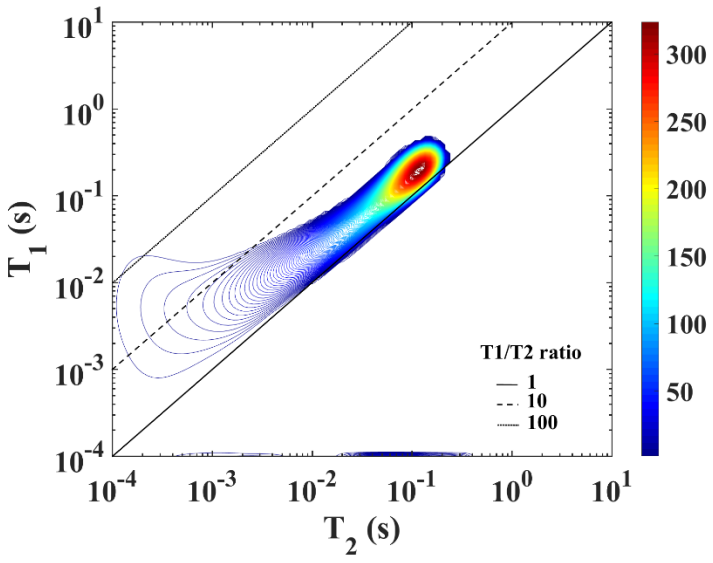

Figure 50 T_1T_2 map of bulk oil 2

Table 7 T_1/T_2 ratio of bulk fluids

Sample	T_2	T_1	T_1/T_2
Brine	2.78	2.78	1
Oil 1	0.135	0.242	1.79
Oil 2	0.120	0.191	1.59

T_1T_2 map of sample 1H fully saturated with brine is shown in Figure 51. Since brine is the only phase inside the pore space, it exhibits surface relaxation and we can see that the predominant peak T_1/T_2 has been shifted above the unity line compared to the bulk water T_1/T_2. Figure 52 and Figure 53 presents the T_1T_2 maps of sample 1H after injection oil until S_{wi} before and after aging, respectively. We see that the predominant peak T_1/T_2 is the same in both figures although individual values of T_1 and T_2 have changed. Brine was injected until S_{or} is reached. Figure 54

shows T_1T_2 maps of sample 1H at S_{or}, which shows the same behavior of fully brine saturated sample. Table 8 summarizes the predominant peak T_1/T_2 values at different saturations for carbonate samples. It is clear that T_1/T_2 value of sample 2H after 7 days aging is higher than that of sample 1H due to additional 1 wt% asphaltene. However, it is difficult to infer wettability from T_1T_2 maps since the water, oil signals overlap, and it is difficult to tell whether the shift above unity is because of asphaltene or it is related to wettability. The solution for this problem is to conduct the T_2-D measurements at the same conditions and then separate oil and water signals. The next step after separating both signals is to use only the brine T_1/T_2 ratio to evaluate wettability since oil T_1/T_2 ratio cannot be used due to the asphaltene presence in the oil. T_1T_2 maps for sample 2H have same issues face in sample 1H and do not have any new observations so the values of T_1, T_2 and T_1/T_2 ratio were only showed in Table 8.

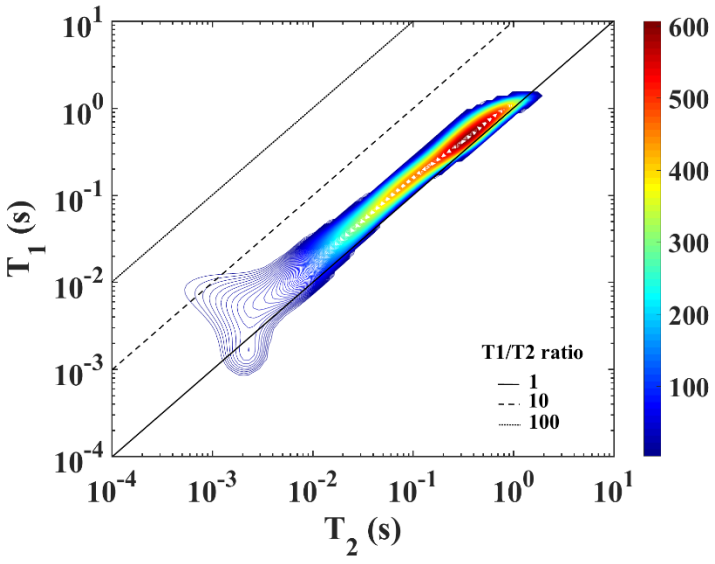

Figure 51 T_1T_2 map of sample 1H at $S_w = 1$

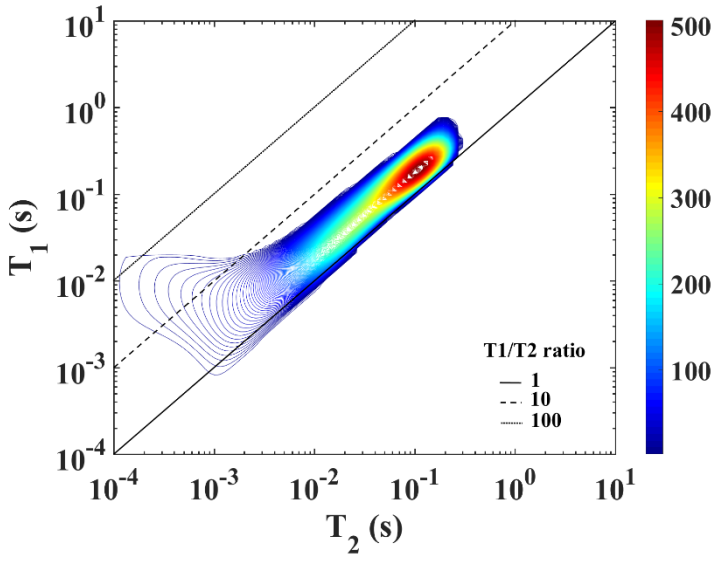

Figure 52 T_1T_2 map of sample 1H at S_{wi} (before aging)

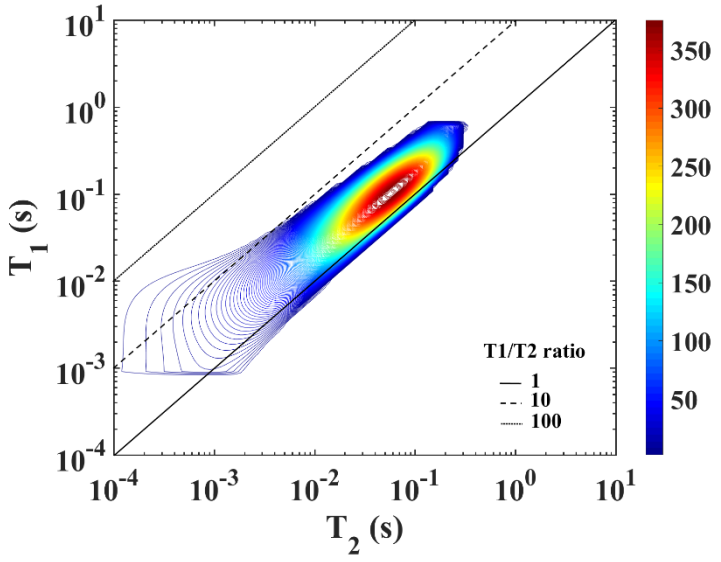

Figure 53 T_1T_2 map of sample 1H at S_{wi} (after 7 days aging)

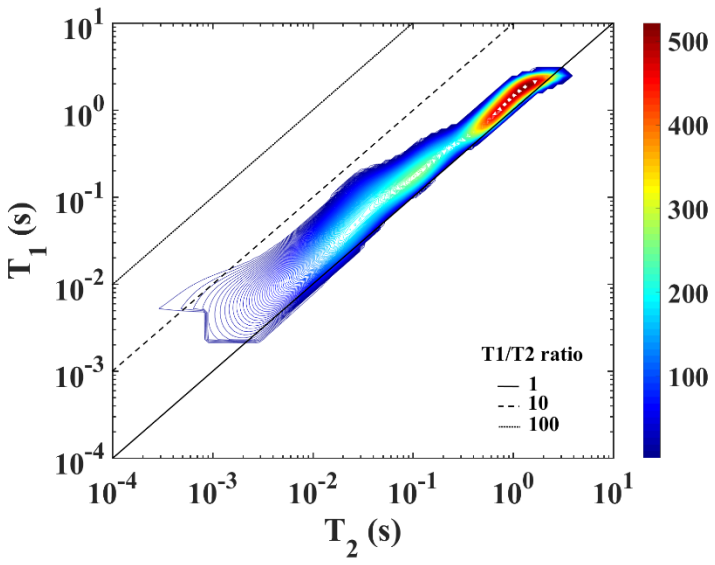

Figure 54 T_1T_2 map of sample 1H at S_{or}

Table 8 Summary of the predominant peak T_1/T_2 values at different saturations for carbonate samples

Sample	$T1/T2_{Sw=1}$	$T1/T2_{Swi}$ (before aging)	$T1/T2_{Swi}$ (7 days aging)	$T1/T2_{Sor}$
1H	1.26	1.79	1.79	1.42
2H	1.26	1.79	2.01	1.26

T_1T_2 map of sample 1S fully saturated with brine is shown in Figure 55. Since brine is the only phase inside the pore space, it exhibits surface relaxation and we can see that the predominant peak T_1/T_2 has been shifted above the unity line compared to the bulk water T_1/T_2. Figure 56 presents the T_1T_2 maps of sample 1S at S_{wi}. Brine was injected until S_{or} is reached. Figure 57 shows T_1T_2 maps of sample 1H at S_{or}, which shows the same behavior of fully brine saturated sample. Sample 2S shows the exact behavior of 1S as shown in Table 9 although oil 2 was used

for sample 2S. This indicates that the added 1 wt% of asphaltene makes no difference without aging. It is difficult to infer wettability from T_1T_2 maps since the water, oil signals overlap, and it is difficult to tell whether the shift above unity is because of asphaltene or it is related to wettability. The solution for this problem is to conduct the T_2-D measurements at the same conditions and then separate oil and water signals. The next step after separating both signals is to use only the brine T_1/T_2 ratio to evaluate wettability since oil T_1/T_2 ratio cannot be used due to the asphaltene presence in the oil.

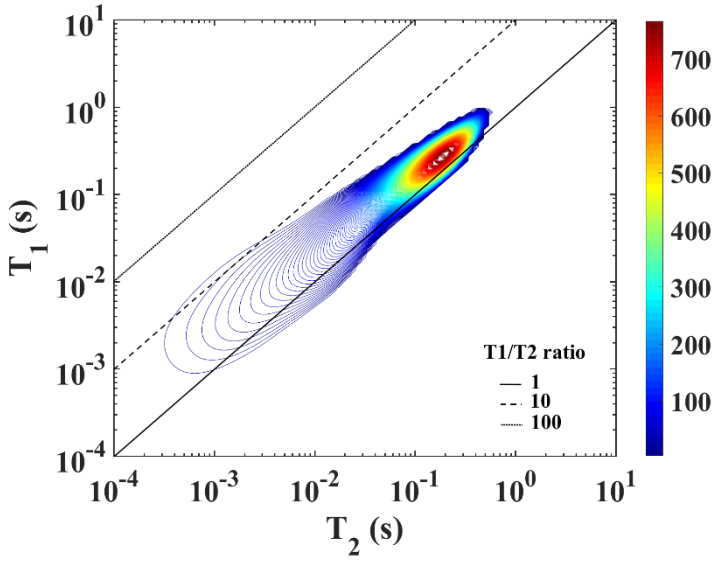

Figure 55 T_1T_2 map of sample 1S at $S_w = 1$

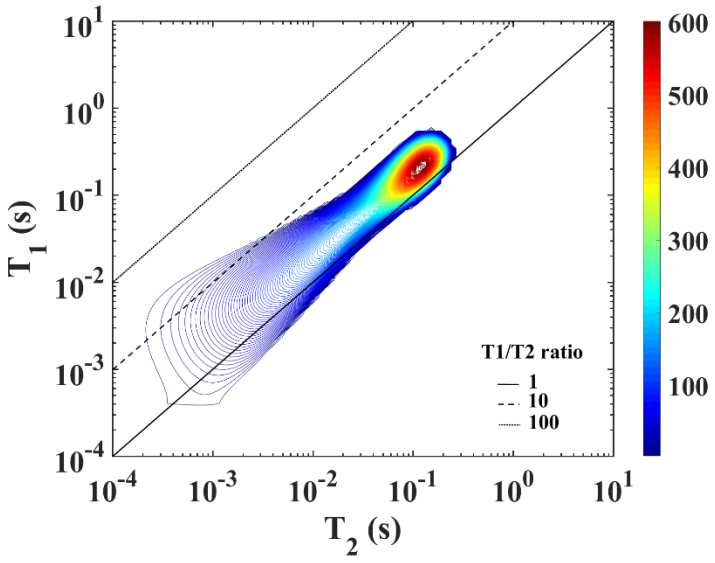

Figure 56 T_1T_2 map of sample 1S at S_{wi}

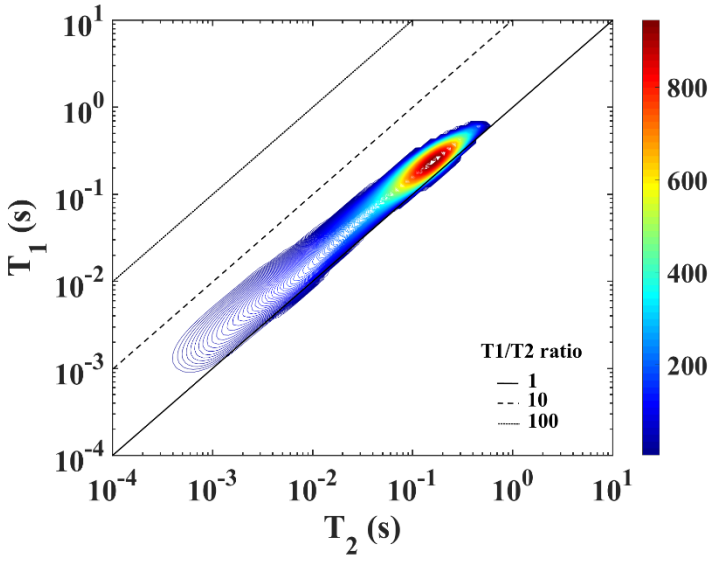

Figure 57 T_1T_2 map of sample 1S at S_{or}

Table 9 Summary of the predominant peak T_1/T_2 values at different saturations for sandstone samples

Sample	$T1/T2_{Sw=1}$	$T1/T2_{Swi}$	$T1/T2_{Sor}$
1S	1.42	1.79	1.42
2S	1.42	1.79	1.42

CHAPTER 5

Conclusions and Recommendations

Wettability is a critical parameter in reservoir description. This is because wettability strongly influences important reservoir quantities and parameters such as relative permeability, residual oil saturation, and capillary pressure curves, which in turns affect the hydrocarbon recovery.

In this work, two different approaches were followed to establish rocks with variable wettability conditions and then NMR measurements were used to evaluate their wettability. In the first approach, Silurian dolomite (SD) and Edward Brown (EB) carbonate samples, that are originally water wet, were chemically treated by Hexadecyl-trimethoxy-silane (HTS) to alter their wettability into oil-wet condition. T_2 and T_1T_2 NMR measurements were conducted to assess rock wettability before and after the treatment. In addition, ultrasonic velocity measurements were run due to the ability of the NMR core holder, developed in UWA, to run NMR and ultrasonic measurements together. In the second approach, T_2 and T_1T_2 NMR measurements were conducted at different saturations on aged carbonate and non-aged sandstone samples saturated with brine and crude oils with different asphaltene content.

The chemical treatment method followed in the first approach was done inappropriately since the two extreme concentrations of Hexadecyl-trimethoxy-silane were used (very high and very low). In addition, the treated samples were not aged to allow the adsorption of the chemical on rock surface to alter wettability. All the above made wettability evaluation using NMR inapplicable. However, in the second approach NMR T_2 measurements predicted wettability conditions very well. T_2 measurements indicate that carbonate samples were strongly water wet

before aging them in oil. After aging, the water wetness has been reduced and they become mixed wet. On the other hand, the sandstone samples showed strong water wetness property. NMR T_1T_2 measurements could not predict wettability due to the existence of asphaltene in oil, which causes deviation of T_1/T_2 ratio above the unity line. If this deviation were related to wettability, it would lead to wrong conclusion. In addition, water and oil signals overlap which imposed another limitation on wettability evaluation using T_1T_2 maps.

It is recommended to choose the proper concentration of the chemical to alter wettability since it could damage the rock if the chemical concentration is too high and it will not cause wettability alteration if concentration is too low. In addition, aging the sample is very important to allow the chemical to be adsorbed on the rock surface and alter its wettability. T_1T_2 maps would not be the appropriate choice to evaluate wettability when oils with high viscosity or containing asphaltene are used. The reason for this is that these types of oil deviates from unity and this could be attributed to wettability leading to wrong conclusion. Thus, it is recommended to use appropriate methods such as T_2-D NMR measurements to separate the oil and water signals. Then wettability can be evaluated using T_1/T_2 of water only. NMR measurements save time, money and effort compared to the available conventional methods. They also do not damage or spoil the rock samples. NMR technology could be extended to be applied in-situ at the field, which would be very commercial and economically feasible.

References

[1] F. F. Craig, *The reservoir engineering aspects of waterflooding*. Richardson, Tex.: Henry L. Doherty Memorial Fund of AIME, 1993.

[2] S. M. Ma, X. Zhang, N. R. Morrow, and X. Zhou, "Characterization of Wettability From Spontaneous Imbibition Measurements," *J. Can. Pet. Technol.*, vol. 38, no. 13, p. 56, Dec. 1999.

[3] W. Anderson, "Wettability Literature Survey- Part 2: Wettability Measurement," *J. Pet. Technol.*, vol. 38, no. 11, pp. 1246–1262, Nov. 1986.

[4] W. G. Anderson, "Wettability Literature Survey Part 5: The Effects of Wettability on Relative Permeability," *J. Pet. Technol.*, vol. 39, no. 11, pp. 1453–1468, Nov. 1987.

[5] W. G. Anderson, "Wettability Literature Survey-Part 6: The Effects of Wettability on Waterflooding," *J. Pet. Technol.*, vol. 39, no. 12, pp. 1605–1622, Dec. 1987.

[6] S. A. Sweeney and H. Y. Jennings, "EFFECT OF WETTABILITY ON THE ELECTRICAL RESISTIVITY OF CARBONATE ROCK FROM A PETROLEUM RESERVOIR," *J. Phys. Chem.*, vol. 64, no. 5, pp. 551–553, May 1960.

[7] E. Sondenaa, F. Bratteli, H. P. Normann, and K. Kollveit, "The Effect of Reservoir Conditions, and Wettability on Electrical Resistivity," in *Proceedings of SPE Asia-Pacific Conference*, 1991, pp. 409–422.

[8] R. J. Suman and R. J. Knight, "Effects of pore structure and wettability on the electrical resistivity of partially saturated rocks—A network study," *GEOPHYSICS*, vol. 62, no.

4, pp. 1151–1162, Jul. 1997.

[9] Y. Han *et al.*, “Experimental investigation on the effect of wettability on rock-electricity response in sandstone reservoirs,” *Fuel*, vol. 239, no. August 2018, pp. 1246–1257, Mar. 2019.

[10] D. Zhou and E. H. Stenby, “A Percolation Study of Wettability Effect on the Electrical Properties of Reservior Rocks,” *Transp. Porous Media*, vol. 29, no. 1, pp. 85–98, Oct. 1997.

[11] E. C. Donaldson, R. D. Thomas, and P. B. Lorenz, “Wettability Determination and Its Effect on Recovery Efficiency,” *Soc. Pet. Eng. J.*, vol. 9, no. 01, pp. 13–20, Mar. 1969.

[12] T. M. Okasha and J. J. Funk, “Fifty Years of Wettability Measurements in the Arab-D Carbonate,” pp. 1–12, 2004.

[13] R. A. Salathiel, “Oil Recovery by Surface Film Drainage In Mixed-Wettability Rocks,” *J. Pet. Technol.*, vol. 25, no. 10, pp. 1216–1224, Oct. 1973.

[14] W. Abdallah *et al.*, “Fundamentals of Wettability,” *Technology*, vol. 38, Jan. 1986.

[15] F. R. Branco and N. A. Gil, “NMR study of carbonates wettability,” *J. Pet. Sci. Eng.*, vol. 157, no. March, pp. 288–294, Aug. 2017.

[16] C. C. Minh *et al.*, “Determination of WETTABILITY from magnetic resonance relaxation and diffusion measurements on fresh-state cores,” in *International Conference and Exhibition, Barcelona, Spain, 3-6 April 2016*, 2016, pp. 211–211.

[17] E. Amott, “Observations Relating to the Wettability of Porous Rock,” *Pet. Trans.*

AIME, vol. 216, pp. 156–162, 1958.

[18] A. S. Al-Muthana, G. G. Hursan, S. M. Ma, A. Valori, B. Nicot, and P. M. Singer, "Wettability As a Function of Pore Size By Nmr," *Soc. Core Anal.*, pp. 1–12, 2012.

[19] W. J. Looyestijn, "Wettability Index Determination From NMR Logs," *Petrophysics*, vol. 49, no. 02, p. 16, 2008.

[20] J. Chen, G. J. Hirasaki, and M. Flaum, "NMR wettability indices: Effect of OBM on wettability and NMR responses," *J. Pet. Sci. Eng.*, vol. 52, no. 1–4, pp. 161–171, Jun. 2006.

[21] M. Fleury and F. Deflandre, "Quantitative evaluation of porous media wettability using NMR relaxometry," *Magn. Reson. Imaging*, vol. 21, no. 3–4, pp. 385–387, Apr. 2003.

[22] R. Freedman, N. Heaton, M. Flaum, G. J. Hirasaki, C. Flaum, and M. Hürlimann, "Wettability, Saturation, and Viscosity From NMR Measurements," *SPE J.*, vol. 8, no. 04, pp. 317–327, Dec. 2003.

[23] G. Q. Zhang, C. C. Huang, and G. J. Hirasaki, "Interpretation of wettability in sandstones with NMR analysis," *Log Anal.*, vol. 41, no. 3, pp. 223–233, 2000.

[24] C. Straley, C. F. Morriss, and W. E. Kenyon, "NMR In Partially Saturated Rocks: Laboratory Insights On Free Fluid Index And Comparison With Borehole Logs," *SPWLA 32nd Annual Logging Symposium*. Society of Petrophysicists and Well-Log Analysts, Midland, Texas, p. 25, 1991.

[25] J. J. Howard, W. E. Kenyon, C. E. Morriss, and C. Straley, "Nmr In Partially Saturated Rocks: Laboratory Insights On Free Fluid Index And Comparison With Borehole

Logs," *Log Anal.*, vol. 36, no. 01, p. 17, 1995.

[26] G. C. Borgia, P. Fantazzini, and E. Mesini, "Wettability effects on oil-water-configurations in porous media: A nuclear magnetic resonance relaxation study," *J. Appl. Phys.*, vol. 70, no. 12, pp. 7623–7625, Dec. 1991.

[27] R. J. S. Brown and I. Fatt, "Measurements Of Fractional Wettability Of Oil Fields' Rocks By The Nuclear Magnetic Relaxation Method," in *Fall Meeting of the Petroleum Branch of AIME*, 1956, p. 4.

[28] R. H. DETTRE and R. E. JOHNSON, "Contact Angle Hysteresis," in *Contact Angle, Wettability, and Adhesion*, vol. 43, AMERICAN CHEMICAL SOCIETY, 1964, pp. 136-144 SE–8.

[29] P. P. Jadhunandan and N. R. Morrow, "Effect of Wettability on Waterflood Recovery for Crude-Oil/Brine/Rock Systems," *SPE Reserv. Eng.*, vol. 10, no. 01, pp. 40–46, Feb. 1995.

[30] R. Akkurt *et al.*, "Nuclear magnetic resonance comes out of its shell," *Oilf. Rev.*, vol. 20, no. 4, pp. 4–23, 2008.

[31] B. Kenyon, R. Kleinberg, C. Straley, G. Gubelin, and C. Morriss, "Nuclear magnetic resonance imaging - technology for the 21st century," *Oilf. Rev.*, vol. 7, no. 3, pp. 19–33, 1995.

[32] M. C. Bowers, R. Ehrlich, J. J. Howard, and W. E. Kenyon, "Determination of porosity types from NMR data and their relationship to porosity types derived from thin section," *J. Pet. Sci. Eng.*, vol. 13, no. 1, pp. 1–14, Apr. 1995.

[33] D. P. Gallegos, D. M. Smith, and C. J. Brinker, “An NMR technique for the analysis of pore structure: Application to mesopores and micropores,” *J. Colloid Interface Sci.*, vol. 124, no. 1, pp. 186–198, Jul. 1988.

[34] W. Yan *et al.*, “Evaluation of wettabilities and pores in tight oil reservoirs by a new experimental design,” *Fuel*, vol. 252, no. December 2018, pp. 272–280, Sep. 2019.

[35] K. Yang *et al.*, “Quantitative Tortuosity Measurements of Carbonate Rocks Using Pulsed Field Gradient NMR,” *Transp. Porous Media*, 2019.

[36] M. D. Hürlimann *et al.*, “Diffusion-editing: New NMR measurement of saturation and pore geometry,” *SPWLA 43rd Annu. Logging Symp. 2002*, no. 2, 2002.

[37] Y. Cai, D. Liu, Z. Pan, Y. Yao, J. Li, and Y. Qiu, “Petrophysical characterization of Chinese coal cores with heat treatment by nuclear magnetic resonance,” *Fuel*, vol. 108, pp. 292–302, 2013.

[38] B. Vincent, M. Fleury, Y. Santerre, and B. Brigaud, “NMR relaxation of neritic carbonates: An integrated petrophysical and petrographical approach,” *J. Appl. Geophys.*, vol. 74, no. 1, pp. 38–58, 2011.

[39] H. Pape, J. E. Tillich, and M. Holz, “Pore geometry of sandstone derived from pulsed field gradient NMR,” *J. Appl. Geophys.*, vol. 58, no. 3, pp. 232–252, Mar. 2006.

[40] Y. Yao and D. Liu, “Comparison of low-field NMR and mercury intrusion porosimetry in characterizing pore size distributions of coals,” *Fuel*, vol. 95, pp. 152–158, 2012.

[41] A. Valori and B. Nicot, “A Review of 60 Years of NMR Wettability,” *Petrophysics – SPWLA J. Form. Eval. Reserv. Descr.*, vol. 60, no. 2, pp. 255–263, Apr. 2019.

[42] I. Shikhov, R. Li, and C. H. Arns, “Relaxation and relaxation exchange NMR to characterise asphaltene adsorption and wettability dynamics in siliceous systems,” *Fuel*, vol. 220, no. September 2017, pp. 692–705, May 2018.

[43] B. Gizatullin, I. Shikhov, C. Arns, C. Mattea, and S. Stapf, “On the influence of wetting behaviour on relaxation of adsorbed liquids – A combined NMR, EPR and DNP study of aged rocks,” *Magn. Reson. Imaging*, vol. 56, no. August 2018, pp. 63–69, Feb. 2019.

[44] S. H. Al-Mahrooqi, C. A. Grattoni, A. K. Moss, and X. D. Jing, “An investigation of the effect of wettability on NMR characteristics of sandstone rock and fluid systems,” *J. Pet. Sci. Eng.*, vol. 39, no. 3–4, pp. 389–398, Sep. 2003.

[45] J. J. Howard, “Quantitative estimates of porous media wettability from proton NMR measurements,” *Magn. Reson. Imaging*, vol. 16, no. 5–6, pp. 529–533, Jun. 1998.

[46] E. Aspenes, A. Graue, and J. Ramsdal, “In situ wettability distribution and wetting stability in outcrop chalk aged in crude oil,” *J. Pet. Sci. Eng.*, vol. 39, no. 3–4, pp. 337–350, Sep. 2003.

[47] H. Westphal, I. Surholt, C. Kiesl, H. F. Thern, and T. Kruspe, “NMR Measurements in Carbonate Rocks: Problems and an Approach to a Solution,” *pure Appl. Geophys. PAGEOPH*, vol. 162, no. 3, pp. 549–570, Mar. 2005.

[48] G. R. Coates, L. Xiao, and M. G. Prammer, “NMR logging,” p. 253, 1999.

[49] M. Flaum and G. Hirasaki, “Fluid and Rock Characterization Using New NMR Diffusion-Editing Pulse Sequences and Two Dimensional Diffusivity-T 2 Maps,” no. September, p. 91, 2003.

[50] H. Y. Carr and E. M. Purcell, “Effects of Diffusion on Free Precession in Nuclear Magnetic Resonance Experiments,” *Phys. Rev.*, vol. 94, no. 3, pp. 630–638, May 1954.

[51] S. Meiboom and D. Gill, “Modified Spin-Echo Method for Measuring Nuclear Relaxation Times,” *Rev. Sci. Instrum.*, vol. 29, no. 8, pp. 688–691, Aug. 1958.

[52] R. D. Majumdar, “A Nuclear Magnetic Resonance Spectropic Investigation of the Molecular Structure and Aggregation Behavior of Asphatenes,” no. December 2015, pp. 1–289, 2015.

[53] D. J. Bell and R. Ballinger, “Inversion recovery sequences,” *Radiopaedia*. [Online]. Available: https://radiopaedia.org/articles/inversion-recovery-sequences?lang=us.

[54] A. Valori and G. Hursan, “Laboratory and Downhole Wettability from NMR T1/T2 Ratio,” *Petrophysics*, vol. 58, no. 04, pp. 352–365, 2017.

[55] L. Cuiec, “Rock/Crude-Oil Interactions and Wettability: An Attempt To Understand Their Interrelation,” in *Proceedings of SPE Annual Technical Conference and Exhibition*, 1984, vol. 1984–Septe.

[56] L. Tipura, “Wettability Characterization by NMR T2 Measurements in Edwards Limestone,” *Dept. Phys. Technol.*, no. 1994, pp. 1–12, 2008.

[57] J. R. Morrow, “Introduction,” *Res. Q. Exerc. Sport*, vol. 67, no. sup3, pp. ii–ii, Sep. 1996.

[58] R. Freedman and N. Heaton, “Fluid characterization using nuclear magnetic resonance logging,” *Petrophysics*, vol. 45, no. 3, pp. 241–250, 2004.

[59] W. J. Looyestijn and J. Hofman, “Wettability Index Determination from NMR Logs,” in *SPE Middle East Oil and Gas Show and Conference*, 2005, vol. 49, no. 2, pp. 130–145.

[60] W. J. Looyestijn and J. Hofman, “Wettability-Index Determination by Nuclear Magnetic Resonance,” *SPE Reserv. Eval. Eng.*, vol. 9, no. 02, pp. 146–153, Apr. 2006.

[61] S. H. Al-Mahrooqi, C. A. Grattoni, A. H. Muggeridge, R. W. Zimmerman, and X. D. Jing, “Pore-scale modelling of NMR relaxation for the characterization of wettability,” *J. Pet. Sci. Eng.*, vol. 52, no. 1–4, pp. 172–186, Jun. 2006.

[62] M. Ghanavati, M.-J. Shojaei, and A. R. S. A., “Effects of Asphaltene Content and Temperature on Viscosity of Iranian Heavy Crude Oil: Experimental and Modeling Study,” *Energy & Fuels*, vol. 27, no. 12, pp. 7217–7232, Dec. 2013.

[63] J. S. Buckley and Y. Liu, “Some mechanisms of crude oil/brine/solid interactions,” *J. Pet. Sci. Eng.*, vol. 20, no. 3–4, pp. 155–160, Jun. 1998.

[64] J. S. Buckley, Y. Liu, and S. Monsterleet, “Mechanisms of Wetting Alteration by Crude Oils,” *SPE J.*, vol. 3, no. 01, pp. 54–61, Mar. 1998.

[65] J. Sayyad Amin, E. Nikooee, S. Ayatollahi, and A. Alamdari, “Investigating wettability alteration due to asphaltene precipitation: Imprints in surface multifractal characteristics,” *Appl. Surf. Sci.*, vol. 256, no. 21, pp. 6466–6472, Aug. 2010.

[66] I. K. Al-Busaidi, R. S. Al-Maamari, M. Karimi, and J. Naser, “Effect of different polar organic compounds on wettability of calcite surfaces,” *J. Pet. Sci. Eng.*, vol. 180, no. May, pp. 569–583, Sep. 2019.

[67] K. A. Rezaei Gomari and A. A. Hamouda, “Effect of fatty acids, water composition and pH on the wettability alteration of calcite surface,” *J. Pet. Sci. Eng.*, vol. 50, no. 2, pp. 140–150, Feb. 2006.

[68] N. R. Morrow, “Wettability and its effect on oil recovery,” *JPT, J. Pet. Technol.*, vol. 42, no. 12, pp. 1476–1484, 1990.

[69] S. T. Dubey and M. H. Waxman, “Asphaltene adsorption and desorption from mineral surfaces,” *SPE Reserv. Eng. (Society Pet. Eng.*, vol. 6, no. 3, pp. 389–395, 1991.

[70] W. G. Anderson, “Wettability Literature Survey-Part 1: Rock/Oil/Brine Interactions and the Effects of Core Handling on Wettability.,” *JPT, J. Pet. Technol.*, vol. 38, no. 11, pp. 1125–1144, 1986.

[71] H. H. Downs and P. D. Hoover, “Enhanced Oil Recovery by Wettability Alteration,” in *Oil-Field Chemistry*, vol. 396, American Chemical Society, 1989, pp. 577–595.

[72] R. T. Johansen and H. N. Dunning, “Relative wetting tendencies of crude oils by capillarimetric method,” United States, 1961.

[73] V. Alipour Tabrizy, R. Denoyel, and A. A. Hamouda, “Characterization of wettability alteration of calcite, quartz and kaolinite: Surface energy analysis,” *Colloids Surfaces A Physicochem. Eng. Asp.*, vol. 384, no. 1–3, pp. 98–108, Jul. 2011.

[74] T. J. M. Ai-aulaqi, “WETTABILITY ALTERATION IN ROCK RESERVOIRS AND ITS EFFECT IN PETROLEUM RECOVERY by,” no. October, 2012.

[75] J. E. Strassner, “Effect of pH on Interfacial Films and Stability of Crude Oil-Water Emulsions,” *J. Pet. Technol.*, vol. 20, no. 03, pp. 303–312, Mar. 1968.

[76] P. R. J. Connolly, J. Sarout, and J. Dautriat, “A NEW APPARATUS FOR COUPLED LOW-FIELD NMR AND ULTRASONIC MEASUREMENTS IN ROCKS AT RESERVOIR CONDITIONS,” in *SPWLA 60th Annual Logging Symposium Transactions*, 2019, pp. 1–9.

[77] O. Toesaeter and M. Abtahi, “Summary for Policymakers,” in *Climate Change 2013 - The Physical Science Basis*, no. December, Intergovernmental Panel on Climate Change, Ed. Cambridge: Cambridge University Press, 2003, pp. 1–30.

[78] J. C. Shaw, P. L. Churcher, and B. F. Hawkins, “The Effect of Firing on Berea Sandstone,” *SPE Form. Eval.*, vol. 6, no. 01, pp. 72–78, Mar. 1991.

[79] D. E. Potts and D. L. Kuehne, “Strategy for Alkaline/Polymer Flood Design With Berea and Reservoir-Rock Corefloods,” *SPE Reserv. Eng.*, vol. 3, no. 04, pp. 1143–1152, Nov. 1988.

[80] R. Freedman, S. Lo, M. Flaum, G. J. Hirasaki, A. Matteson, and A. Sezginer, “A New NMR Method of Fluid Characterization in Reservoir Rocks: Experimental Confirmation and Simulation Results,” *SPE J.*, vol. 6, no. 04, pp. 452–464, Dec. 2001.

[81] K. E. Washburn and Y. Cheng, “Detection of intermolecular homonuclear dipolar coupling in organic rich shale by transverse relaxation exchange,” *J. Magn. Reson.*, vol. 278, pp. 18–24, 2017.

[82] P. M. Singer, D. Asthagiri, Z. Chen, A. Valiya Parambathu, G. J. Hirasaki, and W. G. Chapman, “Role of internal motions and molecular geometry on the NMR relaxation of hydrocarbons,” *J. Chem. Phys.*, vol. 148, no. 16, p. 164507, Apr. 2018.

Vitae

Name	: KAREM ABDULRAHMAN AL-GARADI
Nationality	: Yemeni
Date of Birth	: 12/31/1992
Email	: Karemalgaradi@gmail.com
Address	: DHAHRAN- 31261, SAUDI ARABIA
Academic Background	: B.Sc. Petroleum Engineering, (2012 - 2017), KFUPM, Dhahran, Saudi Arabia. M.S Petroleum Engineering, (2017 - 2019), KFUPM, Dhahran, Saudi Arabia
Published paper	: Not Yet
Submitted paper	: Not Yet